Properties of Rutile (Titanium Dioxide)*

F. A. GRANT

National Bureau of Standards, Washington, D. C.

(Received December 5, 1958)

CONTENTS

1. INTRODUCTION

OXIDE semiconductors, such as rutile, differ from the elemental semiconductors, silicon and germanium, in several respects. Probably the most important is the high melting point, which increases the difficulty of obtaining specimens of high purity. A related effect is the high concentration of vacancies which is "frozen" into the specimens at elevated temperatures. Oxygen vacancies are believed to exceed the cation vacancies in rutile. The formation of an oxygen vacancy in the otherwise pure oxide provides

* Work supported by the U. S. Atomic Energy Commission.

a source of two electrons having an activation energy less than the energy required to raise an electron to the conduction band in the stoichiometric material. Thus the transport properties of the oxide are altered by departures from stoichiometry, just as they are by the presence of impurities.

The second respect in which oxide semiconductors differ from silicon and germanium is the separation of the cations by the oxide ions. This separation leads to a reduction of the overlapping of the cation wave functions. It is undecided whether the wave functions of the cation 3*d* electrons are to be considered as overlapping, or "noninteracting." This question has been discussed by Verwey, *et al.*,[1] Mott,[2] Zener and Heikes,[3] and very recently by Morin.[4] It seems probable that the titanium 3*d* levels (or band) do not overlap the bottom of the much wider 4*s* conduction band. To the extent that electrical conduction is due to 3*d* electrons, one expects a low mobility compared with the electron mobility in silicon and germanium.

Finally, one has the difficulty of distinguishing between chemisorbed oxygen and oxygen from the adjacent bulk material. In other words, our concept of a surface is less precise than in the case of elemental solids.

For these reasons, it is appropriate and timely to examine critically all the available literature on the physical properties of rutile. In the following pages these properties are interpreted in terms of two electronic models. The attempted correlation of the various types of measurement (electrical conductivity, thermopower, etc.) by the use of these models is not satisfactory. It was therefore decided to discuss many physical properties that are not obviously significant from the point of view of the two models.

2. CRYSTAL STRUCTURE

2.1. Introduction

Titanium dioxide exists in three crystalline modifications, rutile, brookite and anatase, all of which have been prepared synthetically. Titanium dioxide precipitated from sulfate or chloride solutions at room temperature is amorphous even after drying at 110°C.[5] At elevated temperatures anatase is precipitated from sulfate solutions, but hydrolysis by direct boiling of chloride solutions produces rutile as the initial crystalline product. Other forms are converted to rutile when heated to temperatures between 700 and 920°C. The transition is not reversible. The stability of anatase is increased by the presence of 0.1% of certain anions.[6] The preparation and mutual transformation of these oxides are discussed in Barksdale.[7]

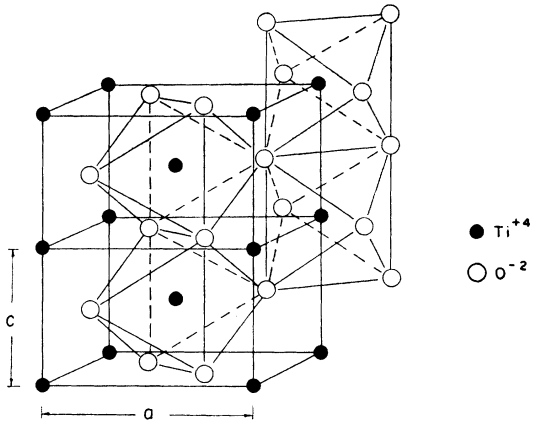

FIG. 1. Crystal structure of rutile (TiO_2). (Courtesy of R. G. Breckenridge, W. R. Hosler, and *The Physical Review*.)

Moore[8] has described the method of preparation of rutile single crystals by the Verneuil flame fusion method. When removed from the furnace the crystals are opaque black because of a slight deficiency of oxygen, but have the rutile crystal structure. After heating in a stream of oxygen the crystals become transparent, with a slight yellow coloration.

2.2. Crystal Structure

The crystal structure of rutile is usually described in terms of an ionic model based on the ions Ti^{4+} and O^{2-}. Although Syrkin and Dyatkina[9] consider that rutile may be regarded as intermediate between ionic and molecular in type, one notes that the Ti—O separation in the O—Ti—O grouping is actually slightly greater than the remaining four Ti—O spacings. This increased separation has been explained[10] as resulting from the repulsion between one oxygen ion and the four equidistant oxygen ions in the same octahedron.

The oxygen ions are arranged in the form of somewhat distorted octahedra (Fig. 1). Each octahedron shares one edge with adjacent members of the chain. Alternatively, the crystal structure may be visualized as chains of ions —O—Ti—O—O—Ti—O. All chains in the same layer are parallel, and the chains in adjacent layers are perpendicular to one another and to the *c* axis.

[1] Verwey, Haayman, and Romeyn, Chem. Weekblad 44, 705 (1948).
[2] N. F. Mott, Can. J. Phys. 34, 1356 (1956); Nuovo cimento Suppl., Ser. 10, 7, 312 (1958).
[3] C. Zener and R. R. Heikes, *Conference on Magnetism and Magnetic Materials*, Boston, Massachusetts, October 16–18, 1956 (Institute of Electrical Engineers, New York, 1957).
[4] F. J. Morin, Bell System Tech. J. 37, 1047 (1958).
[5] Seppo Wilska, Acta Chem. Scand. 8, 1796 (1954) (in English).
[6] H. Knoll and U. Kühnhold, Naturwissenschaften 44, 394 (1957).
[7] Jelks Barksdale, editor, *Titanium, its Occurrence, Chemistry and Technology* (Ronald Press, New York, 1951).
[8] C. H. Moore, Jr., Mining Trans. 184, 194 (1949).
[9] Y. K. Syrkin and M. E. Dyatkina, *The Structure of Molecules and the Chemical Bond* (Butterworths Scientific Publications, London, 1950).
[10] H. Remy, *Treatise on Inorganic Chemistry* (Elsevier Publishing Company, Amsterdam, 1956), Vol. II, p. 59.

2.3. Unit Cell Parameters

The unit cell of rutile is tetragonal. Recent determinations of the cell parameters have been made by Legrand and Delville,[11] and Baur.[12] The values obtained by Baur were $a=4.594\pm0.003$ A, $c=2.959\pm0.002$ A, $c/a=0.6441$, and $x=0.306\pm0.001$. The meaning of the symbol x will be clear from its use in the following section.

2.4. Bond Lengths and Angles

The titanium ions are at the positions (0,0,0) and $(\frac{1}{2},\frac{1}{2},\frac{1}{2})$, and the four oxygen ions are at the positions $\pm(x,x,0)$, and $\pm(\frac{1}{2}+x, \frac{1}{2}-x, \frac{1}{2})$. The bond distances and angles are given in Table I (see also, Fig. 2).

2.5. Interatomic Distances from Ionic Radii

The ionic radii (Zachariasen quoted by Kittel) of the cation and anion are, respectively, $R_C=0.60$ A, and $R_A=1.46$ A.

In ionic crystals, the interatomic distance D_N is given by the relation $D_N=R_C+R_A+\Delta_N$, where N is the coordination number of the cation, and Δ_N is a correction which depends upon N. In rutile the cation has six nearest O^{2-} neighbors, hence $N=6$. From collected crystallographic data of other compounds, Δ_6 is found to be zero, or more correctly, R_C and R_A are calculated on the basis that $\Delta=0$ for $N=6$. The Ti—O separation calculated in this way (2.06 A) is somewhat greater than the observed values (1.944 and 1.988 A), indicating a slight departure from the rule. It is usually assumed that such a discrepancy reflects the contribution of the covalent forces to the crystal bonding.

TABLE I.

Bond	Type[a]	Number of bonds of its type per unit cell	
	(a)		
Ti—O	1	4	1.944±0.004 A
Ti—O	2	2	1.988±0.006 A
O—O	3	8	2.780±0.002 A
O—O	4	2	2.520±0.012 A
O—O	5	2	2.959±0.002 A
Angle	**Bond[a] types**	**Number of angles of its type per unit cell**	
	(b)		
O—Ti—O	1, 1 (smaller angle)	2	80.8°
O—Ti—O	1, 1 (greater angle)	2	99.2°
O—Ti—O	1, 2	8	90.0° (by symmetry)

[a] The numerals refer to the bonds indicated in Fig. 2.

[11] C. Legrand and J. Delville, Compt. rend. **233**, 944 (1953).
[12] W. H. Baur, Acta Cryst. **9**, 515 (1956).

2.6. Other X-Ray Investigations

By the use of Weissenberg photographs, Baur[12] has been able to carry out a Fourier projection of the elementary cell of rutile on the plane perpendicular to [001] (Fig. 3). This figure shows that the electron density does not fall to zero at any point between the oxygen and Ti_{II} ions. The "bridge" between cations and anions is an indication of a covalent contribution to the bonding. These results have been corroborated by the results obtained by a group of Spanish workers.[13,14]

2.7. Madelung Constant

Assuming purely ionic bonding and regular octahedra as the building blocks, Born and Bollnow[15,16] carried out a Madelung calculation for rutile. This analysis predicted a maximum Madelung constant when the axial ratio c/a was equal to 0.721. The observed ratio

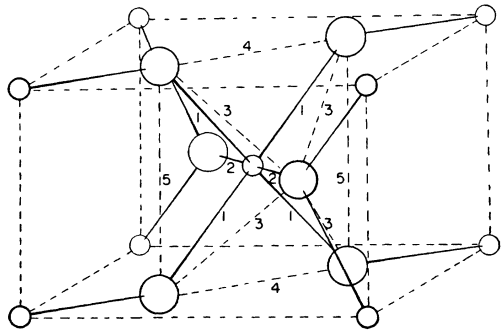

FIG. 2. The atomic arrangement of the tetragonal crystal rutile. Large circles represent oxygen atoms, small circles titanium atoms. The numbers refer to the bond types listed in Table I.

is $c/a=0.6441$. The calculated value of the Madelung constant is 4.816.

Making the assumption that the bonding is completely ionic (based on Ti^{+4} and O^{-2} ions), and taking into account also the repulsive contributions to the total energy, Lennard-Jones and Dent[17] have calculated the expected value of the parameter x (see "Bond Lengths and Angles"). In their method the same fixed separation r was assumed for all six Ti—O bonds, and the potential energy of the crystal was calculated as a function x. The value of the parameter x, necessary to minimize the potential energy was then obtained. Repeating this procedure for a number of values of r, a curve of x *versus* r was plotted. Using the experimental

[13] Bru Villaseca, Cubero, and Vega, Anales real soc. españ. fis. y quim. (Madrid) **46A**, 317 (1950).
[14] M. Cubero and Hernandez Montis, Anales real soc. españ. fis. y quim. (Madrid) **48A**, 133 (1952).
[15] M. Born and O. F. Bollnow, Naturwissenschaften **13**, 559 (1925).
[16] J. E. Lennard-Jones and B. M. Dent, Phil. Mag. **3**, 1204 (1927).
[17] J. E. Lennard-Jones and B. M. Dent, Phil. Mag. **3**, 1204 (1927).

data available at that time, SnO_2 and PbO_2 were found to lie on the theoretical curve. Using Baur's[12] experimental value of $x=0.306\pm0.001$ for rutile, one obtains a value of $r=2.05\pm0.03$ A from the theoretical curve, which is somewhat higher than Baur's experimental value of 1.988 ± 0.006 A. Once again, one finds a discrepancy which probably reflects a covalent contribution to the bonding in rutile.

2.8. Neutron Diffraction

Using thermal neutrons, Shull and Wollan[18] have obtained Laue diffraction patterns of a number of single crystals, including rutile.

3. X-RAY PROPERTIES

3.1. Soft X-Ray Spectra

Confirmation of the band structure theory of solids is obtained from soft x-ray emission experiments. The probability of a transition from an electronic state in a higher band to a vacant lower state depends, among other factors, on the number of electrons in the upper state. Consequently the distribution of intensity with wavelength provides information concerning the density of states as a function of energy.

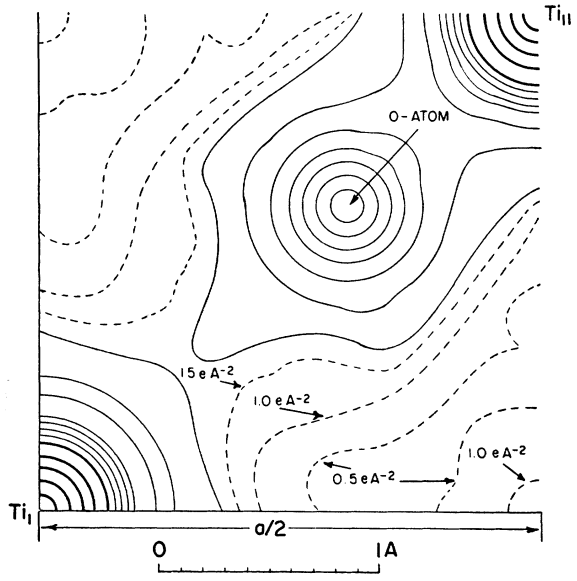

FIG. 3. Fourier projection of rutile on the [001] plane (after W. H. Baur[12]).

Soft x-ray absorption experiments also provide information concerning the energy levels in a solid. The K-absorption edge corresponds to the transition (consistent with the selection rules) of a $1s$ electron to the lowest empty level. Experimental values of the absorption coefficients are plotted against photon energy in Fig. 4.

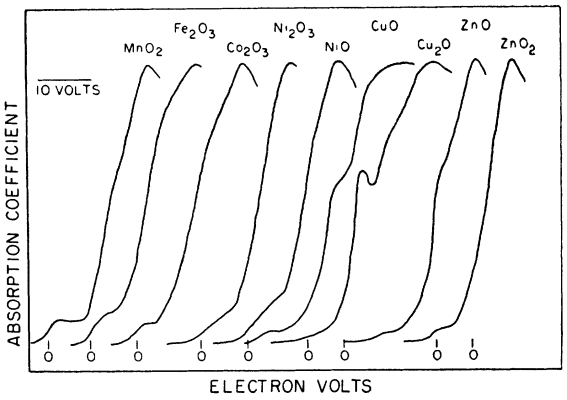

FIG. 4. K-edge structures for oxides of some of the transition metals (after Hanson and Knight[20]).

The distinguishing features of these curves are a small low-energy absorption, followed by a steep rise in absorption coefficient. On the high-energy side of the absorption edge the curve exhibits a fine structure characteristic of the environment of the atom (the type of bonding, etc.).

The shapes of such curves are determined by the absorbing atoms, their immediate surroundings, and by type of structure of which they form a part. Kiestra[19] has summarized his conclusions in the following words:

"(a) In a region close to the edge, the behavior of the absorption coefficient is mainly a property of the atom in question.

"(b) In the following region the fine structure is determined by the immediate surroundings of the atom.

"(c) In the region of highest energy, the fine structure depends essentially on the whole crystal lattice.

"For the transition metals and their compounds (a) comprises the region up to about 40 eV from the edge, (b) the region between about 40 eV and 150 eV, and (c) the region above 150 eV."

Recently, Hanson and Knight[20] have investigated the K-absorption edge structure of the fluorides, oxides, and sulfides of a number of transition metals. These workers found that oxides in which the metal assumed a higher valence exhibited greater low-energy absorption than the same metals in their lower valence form. In highly ionic compounds, the low-energy absorption is less than in compounds between elements exhibiting less difference in electronegativity.

When it is suspected that there is an appreciable change in symmetry and crystal bonding, as in barium titanate at the Curie temperature, the investigation of the K-absorption edge of titanium might prove to be of interest.

[18] C. G. Shull and E. O. Wollan, Naturwissenschaften **36**, 291 (1949).

[19] S. Kiestra, "Conference on the Application of X-ray Spectroscopy to Solid State Problems," University of Wisconsin, Madison, October 23–25, 1950, Report NAVEXOS P-1033, p. 36.

[20] H. P. Hanson and J. R. Knight, Phys. Rev. **102**, 632 (1956).

The fine structure of the K-absorption edge has been investigated for pure titanium,[21,22] titanium and titanium dioxide,[23,24] titanium metal, rutile, anatase, and brookite,[25] and the L-series x-ray spectra of the elements K(19) to Ge(32).[26] A limited interpretation of the experimental results has been given by these authors. Moreover, no attempt has been made to correlate these results with the electron transport properties of these materials. O'Bryan and Skinner[27] have investigated the soft x-ray spectroscopy of many metallic oxides and halides (not including rutile).

3.2. X-Ray Absorption

Brewster[28] lists values of the mass absorption coefficient of rutile. At the wavelengths 0.01, 0.1, 1, and 2 A, the values of the mass absorption coefficient are, respectively, 0.05434, 0.1790, 38.71, and 250.4, respectively. The linear absorption coefficient is equal to the product of the mass absorption coefficient and the density.

4. CRITERIA OF BOND TYPE

4.1. Introduction

When the covalent contribution to the bonding is small, as in the alkali halides, a quantitative estimate of its effect may be made. When a quantitative estimate cannot be made, however, it is usual to make use of certain criteria of covalency, such as the type of crystal structure, atomic radii, bond lengths, position in the periodic table and electronegativity difference of the components, Pauling's rules, etc.

It should be emphasized that the following criteria of the extent of the ionic contribution to the bonding are not necessarily in close agreement. Their value is therefore more qualitative than quantitative in nature.

4.2. Dielectric Constant

The optical and static dielectric constants of covalent crystals are almost equal. In contrast, the static dielectric constant of highly ionic crystals is considerably greater than the optical dielectric constant. The values for rutile single crystals are $K=173$ and $K_{\text{opt}}=8.4$ in the c direction, indicative of a strong ionic character.

4.3. Electronegativity

Mulliken[29–31] defines the electronegativity of an atom as the mean of its ionization potential and its electron affinity, thereby making use of observable quantities. The concept of electronegativity is less precise when more than one valence electron is involved.

Hannay and Smyth[32] have derived a formula which enables the extent of the ionic character of a bond to be estimated from the electronegativities of the bonded partners. This approach yields a value of 43% ionic character for the Ti—O bond in rutile, which is about the same as that of HF and KI.

4.4. Magnetic Susceptibility

The tetravalent titanium and the divalent oxygen ion both have noble-gas configurations. The *temperature-dependent* paramagnetic susceptibility of stoichiometric rutile should therefore be zero, whether the bonding is ionic or covalent. Feeble (Van Vleck) *temperature-independent* paramagnetism, however, is observed, possibly caused by "distortion due to interatomic forces.[33] This distortion is evidence for a departure from ionic bonding, and probably reflects a covalent contribution.

4.5. Bond Lengths

Assuming ionic bonding, but taking into account repulsive forces, Lennard-Jones and Dent (see Sec. 2) have calculated the cation-anion separation in the plane perpendicular to the c axis expected for rutile-type crystals. The measured value of this bond length in rutile is somewhat shorter than the calculated value, and may be taken as evidence for a covalent contribution to the bonding.

4.6. Fourier Projection

Baur has carried out a Fourier projection of the elementary cell of rutile perpendicular to [001] (Fig. 3). For purely ionic bonding one would expect the electron density to fall to zero at some point between the ions.[34] The considerably higher electron density between the oxygen and Ti_{II} ions in Fig. 3 is evidence for a covalent contribution to the bonding.

4.7. Solubility

The low solubility of rutile in polar solvents such as water, is taken as evidence for a considerable covalent contribution to the Ti—O bonding.

[21] Seljakob, Krasnikov, and Stellezkii, Z. Physik **45**, 548 (1927).
[22] G. Okuno, Proc. Phys.-Math. Soc. Japan **18**, 306 (1936).
[23] M. A. Blokhin, Doklady Akad. Nauk. S.S.S.R. **95**, 965 (1954).
[24] V. H. Sanner, Z. Physik **112**, 430 (1939).
[25] I. B. Borovskii, Compt. rend. acad. sci. U.R.S.S. **26**, 764 (1940) (in English).
[26] F. Tyren, Arkiv. Mat. Astron. Fysik **25A**, No. 32 (1937).
[27] H. M. O'Bryan and H. W. B. Skinner, Proc. Roy. Soc. (London) **A176**, 229 (1940).
[28] Gordon F. Brewster, J. Am. Ceram. Soc. **35**, 194 (1952).
[29] R. S. Mulliken, J. Chem. Phys. **2**, 782 (1934); *ibid.* **3**, 573 (1935).
[30] C. A. Coulson, *Valence* (Clarendon Press, Oxford, 1951).
[31] A. F. Wells, *Structural Inorganic Chemistry* (Oxford University Press, New York, 1950).
[32] N. B. Hannay and C. P. Smyth, J. Am. Chem. Soc. **68**, 171 (1946). This formula also appears in references 30 and 31.
[33] L. F. Bates, *Modern Magnetism* (Cambridge University Press, New York, 1951), pp. 44 and 272.
[34] For example, see the projection of the sodium chloride lattice given on page 315 of reference 9.

4.8. Pauling's Rules

One may consider the reduction in stability in the rutile structure resulting from the sharing of one edge by adjacent octahedra (Pauling's third rule[35]) to indicate a departure from purely ionic bonding. This reduction in stability is probably compensated by a corresponding increase in the covalent contribution to the bonding, made possible by this structure.

5. PARAMETERS FOR THE EVALUATION OF EXPERIMENTAL DATA OF SEMICONDUCTORS

5.1. Introduction

It is desirable, whenever possible, to present experimental data in terms of parameters derived from a (more or less simple) model. In the present case, neither the accuracy nor the consistency of the available experimental data permits a choice to be made between the commonly used models. For this reason, the properties of rutile are discussed in terms of two simple models.

In this section, these two models are examined, and the experimentally observed quantities are expressed in terms of such parameters as the ionization potential of the donors, the forbidden energy gap, the effective mass of the electrons, etc. These equations are then used as an indication of the appropriate manner in which to plot the experimental data. In the following sections the experimental data pertaining to the electron transport properties of rutile are introduced, and the parameters derived from these data are given. In a later section, the values of these parameters obtained from magnetic susceptibility, electrical conductivity, thermopower, and other measurements, are summarized. This summary may then be examined for indications of the most satisfactory model to be used in discussing rutile.

It is assumed (as in Fig. 5) that there is a forbidden gap of several electron volts between the valence and conduction bands.[36] Donor sites are believed to lie one- or two-hundred millivolts below the bottom of the conduction band. There may be overlapping of donor wave functions leading to the formation of donor bands. In this case the effective mass is expected to be much higher in the donor band than in the conduction band.

The various symbols used in later sections are defined below:

$n_0=2(2\pi mkT_0/h^2)^{\frac{3}{2}}$ = the constant 2.52×10^{19} electrons/cc and is defined for $T_0=300$°K. This quantity is the so-called "effective number of states."

n_e = the concentration of electrons in the conduction band (per cm³). Electrons in donor bands, which may incidentally contribute to the conduction, are excluded.

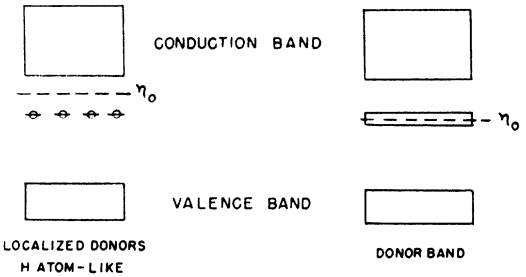

FIG. 5. Two types of band structure assumed in the discussion of the transport properties of rutile.

$M=(m_e/m)$ = the density-of-states effective electron mass.

$t=(T/300)$ = the absolute temperature divided by 300°K.

e = the electronic charge in coulombs.

η = the height of the Fermi level in joules, measured from the bottom of the conduction band.

k = the Boltzmann constant (units depend upon the context-joules per degree when transport properties are in question).

T = the absolute temperature in °K.

N_d = the concentration of donor atoms (per cm³).

E_d = the energy of the donor sites with respect to the bottom of the conduction band, in joules.

b = the electron mobility in cm² volt^{-1} sec^{-1}.

E_g = the energy gap, i.e., the separation of the valence and conduction bands, in joules.

We take the criterion for the applicability of Maxwell-Boltzmann statistics to be $-\eta/kT>3$.

5.2. Donor Sites in Rutile

Nonstoichiometry is believed to result in the presence of oxygen vacancies, together with twice that number of electrons, probably on Ti^{+3} sites.† No distinction will be made between nonstoichiometric rutile and rutile containing pentavalent impurities. In both cases the formation of donor sites will result. The presence of acceptor levels is considered if and when necessitated by experimental evidence. Two cases are considered corresponding to the two models: (a) noninteracting hydrogen-like donor sites, at sufficiently small concentration, in which case a single s electron is considered to move in the field of a net positive charge and (b) interacting donor sites, when the overlapping of the donor wave functions is appreciable. This interaction may lead to the formation of a donor band, and possibly to associations of hydrogen molecule-like donors, or associations of helium-atom-like donors and vacancies, in which two electrons are considered to move in the field of a net positive charge of two.

[35] R. C. Evans, *An Introduction to Crystal Chemistry* (Cambridge University Press, New York, 1952).

[36] W. Crawford Dunlap, Jr., *An Introduction to Semiconductors* (John Wiley & Sons, Inc., New York, 1957).

† The experiments of Gray and McCain indicate that heating of rutile in an atmosphere of hydrogen leads to a loss in weight of the rutile. This result is evidence for the creation of oxygen vacancies rather than hydrogen interstitial atoms. T. J. Gray, *The Defect Solid State* (Interscience Publishers, Inc., New York, 1957), p. 287.

The ground state of the donor sites (or the midpoint of the donor bands) is assumed to lie at an energy level E_d with respect to the bottom of the conduction band (E_d is expected to be a negative number). The simple model of spherical energy surfaces and a single density-of-states mass, is applied to the conduction band. The effective electron mass is assumed to be greater in the donor band than in the conduction band. These models may have to be modified if evidence is found of a second source of electrons (i.e., if oxygen vacancies behave as helium-like centers).

Because of the random distribution of donors, the donor bands may have "tails" so that some overlapping of the conduction band may occur. However, this modification is not introduced into the mathematics because of the obvious difficulties. It can be shown[37] that these models lead to the following results:

$$n_c = n_0 M^{\frac{3}{2}} t^{\frac{3}{2}} \exp(\eta/kT). \tag{5-1}$$

5.2.1. Noninteracting Donor Sites

We usually make the additional assumption that the Fermi level η lies more than $3kT$ higher than the donor impurity levels.‡ This assumption implies that less than one impurity site in twenty is ionized, and leads to the following relation[38]:

$$n_c = \tfrac{1}{2} N_d \exp(E_d - \eta)/kT, \tag{5-2}$$

where N_d = the concentration of donor atoms (per cm^3), and E_d = the energy of the donor sites with respect to the bottom of the conduction band.

If Eqs. (5-1) and (5-2) are combined, one obtains the following expression for the concentration of conduction electrons in terms of the ionization potential of the donor impurity sites[39]

$$n_c = \left(\frac{n_0 N_d}{2}\right)^{\frac{1}{2}} M^{\frac{3}{4}} t^{\frac{3}{2}} \exp E_d/2kT. \tag{5-3}$$

5.2.2. Donor Bands

When the wave functions of the donor sites overlap, the energy levels of the isolated donors must be replaced by bands. Since there are N_d energy levels in the band, and each level may accommodate two of the N_d electrons, the donor band is only half filled at 0°K. Thermal excitations of electrons to the conduction band tend to lower the Fermi level as the temperature is raised. However, it can be shown that the Fermi level remains near the donor band provided that $N_d \gg n_c$. In this case it is appropriate to use the height of the Fermi level η as an indication of the position of the donor band. For this purpose η is expressed in terms of observable quantities by taking logarithms of both sides of Eq. (5-1) and multiplying by kT.

5.3. Interpretation of Hall Data

The Hall constant R for nondegenerate n-type semiconductors (discussed also in Sec. 8) is related to n_c by the relation[40]

$$n_c = r/eR = -6.25 \times 10^{18} r/R. \tag{5-4}$$

The magnitude of the coefficient r, which depends on the type of scattering,[40] lies between 1 and 2.

5.3.1. Noninteracting Donor Sites

Combining Eqs. (5-3) and (5-4) one obtains

$$1/(-R) = \text{constant} \times t^{\frac{3}{2}} \exp(E_d/2kT), \tag{5-5}$$

or

$$[\ln(-R) + \tfrac{3}{4} \ln t] = K_1 - E_d/2kT, \tag{5-6}$$

in which K_1 is a constant which is dependent on M, N_d and on the coefficient r of Eq. (5-4). When the quantity $[\ln(-R) + \frac{3}{4} \ln t]$ is plotted against reciprocal temperature, one obtains $-E_d$ from the slope, and if one knows N_d, and if M is temperature independent, one obtains M from the value of the intercept, K_1, made by this straight line.

5.3.2. Donor Bands

In Sec. (5.2.2) the height of the Fermi level has been discussed in the case in which the overlapping of the donor wave functions leads to the formation of donor bands. Provided that $N_d \gg n_c$, it may be shown that the Fermi level lies below, but near, the midpoint of the donor band. It is reasonable to assume that the electron mobility in the conduction band is much greater than in the donor band. It is therefore appropriate to plot the high temperature Hall data in terms of Eq. (5-1), which may be rewritten with the known quantities on the left-hand side, as follows

$$\ln n_c - \ln n_0 - \tfrac{3}{2} \ln t = \tfrac{3}{2} \ln M + \eta/kT. \tag{5-7}$$

At sufficiently low temperatures, however, as the concentration of conduction electrons decreases, the effect of the electrons in the donor band is expected to dominate. Maxwell-Boltzmann statistics are inapplicable to these latter electrons.

5.3.3. Hall Mobility

The electrical conductivity may be expressed

$$\sigma = n_c e b. \tag{5-8}$$

[37] See Eq. (5.33a) of reference 36.

‡ Because of the high value of the dielectric constant of rutile, E_d may prove to be so small that this assumption is justified only at very low temperatures, and for sufficiently high donor concentrations. The effect of the high dielectric constant will be counteracted to some extent if the effective mass ratio is also high. See p. 267 of reference 36.

[38] The justification for the factor $\frac{1}{2}$ in Eq. (5-2) found in Appendix III of E. Spenke, *Elektronische Halbleiter* (Springer-Verlag, Berlin, 1956).

[39] Apart from the factor 2, and the sign of E_d, this is Eq. (5-31) of reference 36. E_d, of course, is measured with respect to the bottom of the conduction band.

[40] Figure 6.5 of reference 36.

Combining Eqs. (5-4) and (5-8) one obtains an expression for the mobility b in terms of the Hall coefficient and the electrical conductivity σ:

$$b=0.84\sigma(-R/r). \tag{5-9}$$

5.4. Interpretation of Electrical Conductivity Data

5.4.1. *Intrinsic Semiconductors*

If the density-of-states masses of electrons and holes are equal, then the Fermi level is in the middle of the energy gap, i.e., $\eta=-E_g/2$. Combining Eqs. (5-1) and (5-8) and

$$\sigma=n_0ebM^{\frac{3}{2}}t^{\frac{3}{2}}\exp(-E_g/2kT). \tag{5-10}$$

In this case the temperature dependence of the exponential factor is usually so great in comparison with that of the factors b and $t^{\frac{3}{2}}$ that Eq. (5-10) may be written

$$\sigma=K_2\exp(-E_g/2kT). \tag{5-11}$$

E_g may then be evaluated from the slope of a plot of $\ln\sigma$ *versus* reciprocal temperature.

5.4.2. *Impurity Semiconductors*

Isolated donors.—In the case of noninteracting impurities, one combines Eqs. (5-3) and (5-8) to give

$$\ln\sigma=\tfrac{1}{2}\ln(n_0N_d/2)+\ln e+\ln b+\tfrac{3}{4}\ln M+\tfrac{3}{4}\ln t+\exp(E_d/2kT). \tag{5-12}$$

Without some assumption concerning the temperature dependence of the mobility b, E_d cannot be evaluated from conductivity data alone. (The assumption of a single density-of-states electron mass for the conduction band necessarily implies that M is considered to be temperature independent.)

Breckenridge and Hosler[41] (following Fröhlich[42,43]) attempt to interpret their data by using the following relation for the mobility when the scattering is predominantly due to optical lattice vibrations:

$$b=A(\exp(\theta/T)-1), \tag{5-13}$$

where θ is the Debye temperature. After the appropriate substitution

$$\ln\sigma-\tfrac{3}{4}\ln t-\ln(\exp(\theta/T)-1)=K_3+(E_d/2kT), \tag{5-14}$$

in which K_3 is a constant which depends on N_d, A, and M. An assumption concerning the value of θ permits the left-hand side of Eq. (5-14) to be evaluated from conductivity measurements, and plotted against reciprocal temperature. From the slope E_d may be determined. Since K_3 is dependent on the unknowns N_d, A, and M, it is not feasible to attempt an interpretation of the intercept of this plot in the absence of further information.

Actually, (as shown in Sec. 8) the Hall mobility data of Breckenridge and Hosler for slightly reduced rutile are adequately represented above room temperature by the empirical relation

$$b=aT^{-2.5}, \tag{5-15}$$

where T is the absolute temperature, and a is a constant independent of temperature. Substitution of this relation into Eq. (5-12) enables one to write

$$\ln\sigma+1.75\ln t=K_4+E_d/2kT. \tag{5-16}$$

Donor bands.—At sufficiently low temperatures the electrons would be expected to lie in the donor band. The donor-band conductivity in this low-temperature range should depend on temperature chiefly through the mobility factor b. Little information would be obtainable concerning the position of the donor band with respect to the conduction band.

At higher temperatures the electrons in the conduction band should make a greater contribution to the conductivity than the electrons in the donor band. Provided that information is available concerning the electron mobility, the data on electrical conductivity at higher temperatures may be used to give information concerning the Fermi level, and hence the approximate position of the donor band. Making the usual assumptions concerning the applicability of Maxwell-Boltzmann statistics and of the concept of a single effective electron mass to the electrons in the conduction band, we may combine Eqs. (5-1) and (5-8) to yield the following relation:

$$\ln\sigma-\ln n_0e-\tfrac{3}{2}\ln t=\tfrac{3}{2}\ln M+\ln b+\eta/kT \tag{5-17}$$

in which the quantities on the left-hand side are all known. When the assumption implied in Eq. (5-13) is valid, we may combine Eqs. (5-13) and (5-17) and express the result in the form

$$\ln\sigma-\tfrac{3}{2}\ln t-\ln(\exp(\theta/T)-1)=K_5+\eta/kT. \tag{5-18}$$

When the $T^{-2.5}$ relation [Eq. (5-15)] is valid, one may write

$$\ln\sigma+\ln t=K_6+\eta/kT. \tag{5-19}$$

5.5. Interpretation of Thermopower Data

5.5.1. *Impurity Semiconductors*

Noninteracting donors.—Equating Eqs. (5-1) and (5-2) one obtains

$$n_0M^{\frac{3}{2}}t^{\frac{3}{2}}\exp(\eta/kT)=\tfrac{1}{2}N_d\exp(E_d-\eta)/kT \tag{5-20}$$

which may be expressed in the form

$$\tfrac{1}{2}\ln n_0+\tfrac{3}{4}\ln M+\tfrac{3}{4}\ln t+\exp(\eta/kT)=\tfrac{1}{2}\ln N_d+E_d/2kT-\ln 2. \tag{5-21}$$

Noting that

$$\eta/kT=eQ/k+Q^*/kT \tag{5-22}$$

[41] R. G. Breckenridge and W. R. Hosler, Phys. Rev. **91**, 793 (1953).
[42] H. Fröhlich and N. F. Mott, Proc. Roy. Soc. (London) **A171**, 496 (1939).
[43] Fröhlich, Pelzer, and Zineau, Phil. Mag. **41**, 221 (1950).

[see Eq. (7-2)], where Q^* is approximately equal to $2kT$, one obtains

$$eQ/k+\tfrac{3}{4}\ln(T/300)=K_7+E_d/2kT \qquad (5\text{-}23)$$

in which the constant K_7 includes Q^*/kT, and the impurity concentration term, and the effective mass term, which are assumed to be temperature independent. The thermopower, Q, is defined in Sec. 7.1.

Donor bands.—At sufficiently low temperatures, the contribution of the electrons in the conduction band is negligible. In this temperature region, the electrons in the donor band are expected to exhibit degeneracy, and the dynamic term Q^*/kT of Eq. (5-22) should make the major contribution to the thermopower. This contribution (approximately $2k/e$) is almost temperature independent.

At higher temperatures, where the electrons in the conduction band make the main contribution to the thermopower, the height of the Fermi level is related to the thermomower through Eq. (5-22). Replacing Q^* by its approximate value $2kT$, one obtains

$$E_f=\eta/e=(Q+2k/e)T. \qquad (5\text{-}24)$$

Thus when the donor sites interact to form donor bands one expects an almost temperature-independent value for QT in the higher temperature range. At still higher temperatures where thermal excitation raises a large proportion of the electrons from the donor band to the conduction band, the Fermi level falls below the donor band with increasing temperature, and Q should tend to a constant value.

5.5.2. *Correlation of Thermopower and Conductivity Data*

Impurity semiconductors.—When the temperature is sufficiently high for the contribution of the electrons in the conduction band to dominate the contribution to the conductivity of the electrons in the donor band, the correlation between thermopower and conductivity data is independent of the interaction between donor sites. Equations (5-1) and (5-8) may be combined to yield

$$\ln\sigma=\ln(n_0e)+\ln b+\tfrac{3}{2}\ln M+\tfrac{3}{2}\ln t+\eta/kT. \qquad (5\text{-}25)$$

When the foregoing assumption, Eq. (5-13), concerning b is permissible, one obtains

$$\ln\sigma-\tfrac{3}{2}\ln t-\ln(\exp(\theta/T)-1)=K_8+\eta/kT \qquad (5\text{-}26)$$

in which K_8 is a constant which depends on A and M. The thermopower Q may be expressed in the form $Q=(\eta-Q^*)/eT$, where Q^* is a quantity of the order of magnitude of $2kT$.§ Whence

$$\ln\sigma-\tfrac{3}{2}\ln t-\ln(\exp(\theta/T)-1)=K_8+(eQ/K)+Q^*/kT. \qquad (5\text{-}27)$$

If an assumption is made concerning θ, the left-hand side of this equation may be evaluated from conductivity measurements. However, the quantity K_8 involves both the effective mass ratio M and the mobility factor A. Hence, in the absence of further information, no correlation between electrical conductivity and thermopower is possible.‖ To the extent that the term Q^*/kT is temperature independent, however, it should be possible to correlate dQ/dT with the rate of change of the left-hand side with temperature.

A similar conclusion is reached when the mobility b is inversely proportional to a power of the absolute temperature, as in Eq. (5-15).

5.5.3. *Correlation of Thermopower and Hall Data*

Correlation of thermopower Q with the Hall coefficient would involve one fewer variable (b), and would therefore be preferable to the correlation with electrical conductivity.

6. ELECTRICAL CONDUCTIVITY

6.1. Rutile Single Crystals (Intrinsic)

Cronemeyer[44] has measured the intrinsic conductivity of rutile single crystals in the temperature range 300° to 1400°C, using specimens approximately 1×1×10 mm in dimensions. The four-terminal method of measurement was used (see his Fig. 3); hence, the measured conductivity should be independent of the electrode material. However, the conductivity was found to be field dependent when the field strength was greater than 10 v/cm for the intrinsic conductivity, and greater than 0.1 v/cm for reduced (presumably nonstoichiometric) samples.

Cronemeyer's results may be represented by the following equations, in which σ represents the electrical conductivity in (ohm cm)$^{-1}$, and T is the absolute temperature:

Direction perpendicular to the c axis

623° to 1123°K

$$\ln\sigma=7.92-17\,600/T \qquad (6\text{-}1)$$

1123° to 1673°K

$$\ln\sigma=11.10-21\,200/T. \qquad (6\text{-}2)$$

Direction parallel to the c axis

773° to 1223°K

$$\ln\sigma=8.43-17\,600/T \qquad (6\text{-}3)$$

1223° to 1673°K

$$\ln\sigma=11.30-21\,200/T. \qquad (6\text{-}4)$$

§ References are given in Sec. 7.

‖ However, in some materials, such as NiO, it is possible to equate the density of states with the number of cations. This simplification, which results from the localization of the cation wave functions, facilitates a correlation of thermopower and conductivity data without requiring a knowledge of the effective electron mass. See F. J. Morin, Bell System Tech. J. 37, 1047 (1958).

[44] D. C. Cronemeyer, Phys. Rev. 87, 876 (1952).

The respective activation energies calculated from these data are 1.53, 1.84, 1.53, and 1.84 ev. For intrinsic samples, the energy gaps are assumed to be approximately twice these values. In deriving these results the temperature variation of the $(T/300)^{\frac{3}{2}}$ and mobility factors of Eq. (5-1) have been neglected.

Cronemeyer associates the 3.06-ev energy gap obtained in this manner with the optical absorption edge at 3.02 ev.

A more recent investigation of the conductivity of single crystals of rutile has been carried out by Y. L. Sandler.[45] Preliminary published results indicated a somewhat higher conductivity in the temperature range 250° to 700°C, and a somewhat smaller energy gap of 2.8 ev.

6.1.1. Field Strength Dependence

Below 900°C, Cronemeyer's measurement[44] of the intrinsic conductivity of rutile showed some field strength dependence for fields greater than 10 v/cm. Measurements made at 820°C showed an increase in conductivity of about fifty percent when the field was increased to about 20 v/cm. Nonlinearity apparently begins at an even lower field strength (0.1 v/cm) in reduced samples.

6.1.2. Current versus Time

Sandler[45] has observed the current *versus* time characteristics of rutile single crystals. Measurements were made at temperatures up to 720°C for various applied steady voltages. Only curves for 654°C are given in the report. Although it was not explicitly stated, the two-terminal method was probably used, with evaporated gold electrodes. The discussion seems to indicate that the specimens were in an atmosphere of pure oxygen. To ensure that the observed time-dependent effects were not due to surface conduction, a guard-ring electrode was used.

The curves were characterized by relaxation times that decreased as the applied voltage increased. For 1.06-v potential difference, the relaxation time was about two minutes. The author considered that the data might be explained in terms of space-charge polarization and field emission.

6.1.3. Ionic Conductivity

Large currents could be passed through the rutile crystals for hours without destructive effect. Hence Cronemeyer concluded that the conductivity of rutile was essentially electronic.

6.1.4. Dependence on Area of Cross Section

The conductivity was observed to increase by a factor of fifteen when the cross-sectional area was increased from 3×10^{-2} to 6×10^{-2} cm^2. Cronemeyer suggested the possibility that this was due to "carrier injection with predominant recombination at the surface."

6.1.5. Other Phenomena

Sandler[45] has investigated the effect on the conductivity of rutile crystals of the heating during the process of depositing the evaporated gold electrodes. Electrodes were formed at 100 and 300°C. The conductivity ceased to be an exponential function of reciprocal temperature below 270°C, and below 500°C, respectively.

In the presence of water vapor, the conductivity was considerably increased. By the use of a guard electrode, it was shown that the effect was not due to surface conduction, but was probably due to the effect of moisture on the crystal-electrode interface.

6.2. Rutile Ceramic (Intrinsic)

Dependence of electrical conductivity on oxygen pressure is probably associated with departures from stoichiometry.¶ The conductivity of rutile containing intentionally introduced oxygen vacancies is discussed in a later section. The workers referred to in this section made no deliberate attempt to reduce their specimens more than the degree of reduction incidental to the conditions of measurement.

Earle[46] measured the electrical conductivity of pressed disks of rutile as a function of the pressure of the surrounding oxygen. His results may be expressed in the form

$$\ln\sigma = A - B\ln p, \tag{6-5}$$

where σ is the conductivity in (ohm cm)$^{-1}$, p is the oxygen pressure in atmospheres, and A and B are temperature dependent parameters.

At pressures below 30 mm of mercury B was found to be $\frac{1}{2}$ at 626°C, and equal to $\frac{1}{3}$ in the temperature range 755° to 968°C. Above 30 mm of mercury, B was equal to $\frac{1}{4}$. At 50 mm of mercury and 1000°K the conductivity was 1.6×10^{-6} (ohm cm)$^{-1}$. The activation energy was about 1.7 ev, and appeared to be independent of the oxygen pressure. Evaporated gold electrodes were used.

Earle investigated the possibility of ionic conductivity, and believes that its contribution was negligible under the conditions of his experiment.

Hauffe[47] also investigated the dependence of the electrical conductivity of rutile on the pressure of the surrounding oxygen gas. His results may be expressed by the same formula, but with different values of A

[45] Laboratory for Insulation Research, Massachusetts Institute of Technology, Progress Rept. No. XVII (1955).

¶ The effect of oxygen pressure on surface conductivity is also important. The effects of oxygen and other gases on the surface conductivity of silicon and germanium are discussed in *Semiconductor Surface Physics*, R. H. Kingston, editor (University of Pennsylvania Press, 1956).

[46] Marshall D. Earle, Phys. Rev. **61**, 56 (1942).

[47] K. Hauffe, *Reaktionen in und an festen Stoffen* (Springer-Verlag, Berlin, 1955), p. 136.

and B. At 800°, 900°, and 1000°C, the values of B were, respectively, 1/4.8, 1/4.4, and 1/5.3.

Combining measurements made at these three temperatures, and using the approximate value of $\frac{1}{5}$ for B, Hauffe's results may be represented roughly by the relation

$$\ln\sigma \doteq -\tfrac{1}{5}\ln p - 22\,400/T \qquad (6\text{-}6)$$

in which p is expressed in atmospheres, and T is the absolute temperature. The coefficient of $1/T$ yields an activation energy of 1.93 ev.

Gorelik[48] has measured the electrical conductivity of "pure" sintered rutile, and rutile to which various amounts of the oxides of the alkaline earths had been added. His results for "pure" rutile may be expressed by the following formula in the temperature range 380° to 490°K:

$$\ln\sigma = 2.5 - 11\,700/T. \qquad (6\text{-}7)$$

The corresponding activation energy is 1.02 ev. Gorelik's investigation of the effect of a magnetic field on the electrical conductivity is discussed in another section.

6.3. Reduced Rutile

The term "reduced rutile" is used here to signify that an attempt has been made to introduce oxygen vacancies by heating the specimen in oxygen at reduced pressure, or in an atmosphere of hydrogen or some other reducing gas. It is implied that the specimens have been quenched so that the vacancy concentration is higher than that corresponding to the equilibrium at the temperature and pressure at which measurements are made.

When an oxygen vacancy is created, the two electrons associated with the ion must be retained in the crystal to preserve electrical neutrality. There is some uncertainty whether these electrons (a) are associated with the oxygen vacancies to form helium-like donor sites, or (b) whether the electrons convert two Ti^{+4} sites into Ti^{+3} sites.

In case (a) one, or possibly two, activation energies are expected for electron transport phenomena when the vacancy concentration is too low for the formation of impurity bands. Because of the formation of donor bands one expects the disappearance of the activation energy at sufficiently low temperatures when the vacancy concentration is high.

6.3.1. Experimental Results

Breckenridge and Hosler[49] measured the electrical conductivity of reduced rutile single crystals and ceramics. The conductivity of these samples lay in the range 0.03 to 10 (ohm cm)$^{-1}$, depending on the degree of reduction, which was carried out in hydrogen at elevated temperatures.

The curves of the logarithm of the conductivity *versus* reciprocal temperature were fairly flat, and in most cases had negative slopes at 1000 and at 77°K.

There are so many disposable parameters in the simple model [Eq. (5-12)] (Debye temperature θ, impurity concentration, effective mass, etc.) that it is unlikely that its use in the interpretation of these data can yield significant information, except in conjunction with Hall data. The values of the electron mobility obtained from Breckenridge and Hosler's conductivity and Hall data are discussed in Sec. 8.

Kataoka and Suzuki[50] have made measurements of the electrical conductivity and thermopower on reduced rutile ceramic. When these results are plotted[51] according to Eq. (5-16) assuming isolated donor levels, the slopes correspond to values of the donor ionization potentials in the range 0.29 to 0.35 ev. An exception to this result (0.23 ev) was the sample of highest conductivity (20 ohm^{-1} cm^{-1}) for which the explanation could be partial degeneracy.

When the results are plotted[51] according to Eq. (5-19) assuming a donor band, the resulting values of the Fermi level lie in the range 0.12 to 0.15 ev, with the exception of the sample of highest conductivity which yielded a value of 0.09 ev.

Boltaks[52] and co-workers have investigated the conductivity of sintered specimens of rutile which had been reduced in hydrogen or in carbon monoxide. They found that the temperature variation of the pre-exponential term in Eq. (5-12) could not be neglected. When allowance was made for the $T^{\frac{3}{2}}$ factor in Eq. (5-12) a linear plot of $\ln\sigma$ *versus* reciprocal temperature was obtained. From the slope of the tangent to this curve, the ionization potential E_d of the donor sites was estimated to be less than 0.2 ev at room temperature. Apparently no consideration has been given to the effect of the variation of the mobility b with temperature [Eq. (5-12)].

6.3.2. Single Crystals versus Ceramics

The measurements of Breckenridge and Hosler[49] may be examined to compare the properties of polycrystal-

[48] S. I. Gorelik, J. Exptl. Theoret. Phys. U.S.S.R. **21**, 826 (1951).

[49] R. G. Breckenridge and W. R. Hosler, Phys. Rev. **91**, 793 (1953).

[50] S. Kataoka and T. Suzuki, Bull. Electrotech. Lab. Tokyo **18**, 732 (1954).

[51] Measurements of electrical conductivity made by Kataoka and Suzuki may be represented within the experimental error by the following expressions between $1000/T = 1.5$ and $1000/T = 3.5$:

Specimen	$\log_{10}\sigma$
1	$2.12 - 250/T$
2	$2.02 - 550/T$
3	$1.72 - 520/T$
4	$1.40 - 500/T$
5	$0.60 - 400/T$
6	$-0.13 - 475/T$

In the same temperature range, $\log t = \log(T/300)$ may be represented approximately as a function of $1/T$ by the expression $0.62 - 184/T$. Substitution of these expressions into Eqs. (5-16) and (5-19) yields the activation energies and ionization potentials given in the text. The mobility has been assumed to be proportional to $T^{-2.5}$ (see Sec. 8-2).

[52] Boltaks, Vasenin, and Salunina, Zhur. Tekh. Fiz. **21**, 532 (1951).

TABLE II. Comparison of parameters for single crystals and ceramics reduced in hydrogen under approximately the same conditions (from Table I of Breckenridge and Hosler[a]).

	Reduction temperature °C	Reduction time in minutes	Resistivity at 300°K ohm-cm	Hall coefficient at 300°K $(-R)$	Activation energy ΔE_2 ev[b]	n_2[b]	Effective mass ratio of electrons m_e/m
National Lead single crystal	800	5	8	4	0.12	1.4×10^{19}	43
National Bureau of Standards ceramic	800	5	1	0.3	0.14	29×10^{19}	55
Linde single crystals	800	indefinite	0.7	0.10	0.16	15×10^{20}	46
(c direction)							
(a direction)	800	15	1	0.10	0.15	13×10^{20}	114
National Bureau of standards ceramic	800	average of 5, 10, 20 min specimens[c]	1	0.50	0.14	3.1×10^{20}	60

[a] See reference 49.
[b] See Eq. (8-2).
[c] The corresponding resistivity and Hall curves are almost coincident.

line specimens and single crystals. When this comparison is made for specimens that have been reduced under similar conditions, there is no evidence for a significant difference between the single crystal and polycrystalline specimens with respect to mobility, effective mass, or activation energy.

In Table II some of Breckenridge and Hosler's results have been tabulated for the purpose of comparing the parameters for single crystal and ceramics. The comparison is justified only for pairs of samples that had been reduced (in hydrogen) at the same temperature for approximately the same length of time.

As an example of the difficulty of interpreting these results, one notes that the Hall coefficient of the National Lead single crystal (reduced 5 min at 500°C) is higher (by a factor of eight) than that of the ceramic specimen subject to the same reduction. However, the Hall coefficient of the Linde crystal is less than or equal (depending on the direction of the current with respect to the optical axis) to that of the ceramic specimen. Similarly, there appears to be no evidence that the effective mass ratio is greater for single crystals than for ceramic specimens.

6.4. Rutile Containing Added Impurities

6.4.1. Conductivity in Air at Normal Pressure

The effect of impurities on the electrical conductivity of rutile ceramics has been investigated by Hauffe,[47,53] by Grunewald,[54] and by Johnson.[55]

Johnson's samples were air-quenched from 1200 to 250°C and measurements were made at the latter temperature. The results should be accepted with some caution because little attention was paid to the state of reduction of the specimens, and the impurities may have assumed valences other than those expressed in the formulas given. In every case the effect of the impurity approached a saturation value when the concentration exceeded about one or two mole percent. This saturation value is given in the following summary.

6.4.2. Impurities of the Type X_2O

The oxides of lithium, potassium, and silver decreased the conductivity of rutile, while that of sodium produced an increase (Table III). The effect was small in comparison with some of the results discussed in the following.

6.4.3. Impurities of the Type XO

The effects of admixture of the oxides of beryllium, magnesium, calcium, strontium, barium, zinc, cadmium,

TABLE III. Effect of various impurities[a] on electrical conductivity of rutile ceramic at 250°C (after Johnson[b]).

Impurity	Change in conductivity	Impurity	Change in conductivity
WO_3	×4000		
MoO_3	×0.5		
P_2O_5	×1020	BeO	×25
Sb_2O_5	×833	MgO	×0.5
V_2O_5	×27	CaO	×0.07 (?)[c]
Ta_2O_5	×4166	SrO	×0.25
Nb_2O_5	×5500	BaO	×0.95
		ZnO	×0.33
SiO_2	×3.3	CdO	×0.50
ZrO_2	×0.9	NiO	×0.33
B_2O_3	×6	CoO	×0.33
Al_2O_3	×0.4	Li_2O	×0.07
Fe_2O_3	×0.5	Na_2O	×1.7
Cr_2O_3	×3.5	K_2O	×0.7
Ga_2O_3	×0.4	Ag_2O	×0.7
Y_2O_3	×0.1		

[a] "Saturation" effect—usually about one mole percent impurity.
[b] See reference 55.
[c] See text.

[53] Hauffe, Grunewald, and Tränckler-Greese, Z. Elektrochem. **56**, 937 (1952).
[54] H. Grunewald, Ann. Physik **14**, 121 (1954); Hauffe, reference 47.
[55] G. H. Johnson, J. Am. Ceram. Soc. **36**, 97 (1953).

nickel, and cobalt were investigated. The effect was small, except in the case of beryllium (increase by a factor of 25), and calcium (decrease by a factor of 0.07). The effect of beryllium was considered to be possibly due to the donor electrons resulting from the formation of interstitials. In the case of calcium the explanation of the anomalously low value may be as follows. Comparison of Johnson's Table IV with his Fig. 1 suggests that the correct value for calcium is probably considerably higher than 0.07, a value which was apparently influenced by one low experimental point.

Gorelik[56] has investigated the effect of various concentrations of the oxides of the alkaline earths on the electrical conductivity of rutile in the temperature range 380° to 490°K. Values of the activation energies obtained from plots of the logarithm of the conductivity *versus* reciprocal temperature lay in the range 0.78 to 1.15 ev for additions of CaO and SrO. At a temperature of 418°K the admixture of about three moles of CaO per hundred moles of TiO_2 caused a fourfold increase in conductivity. Further increase in CaO content caused the conductivity to decrease until it reached one quarter of its initial value when the CaO content reached twenty-five moles per hundred moles of TiO_2.

One mole of SrO per hundred of TiO_2 yielded a fifty-fold increase in conductivity over the value for "pure" rutile. Further admixture of SrO caused a decrease in conductivity, so that an admixture of 50 moles of SrO per 100 moles of TiO_2 resulted in a value of conductivity only slightly higher than the value for "pure" rutile. Gorelik interpreted his results in terms of contributions from ionic and electronic conductivity. This interpretation was based partly on his investigation of the effect of a magnetic field on the conductivity of these specimens, and is discussed further in another section.

6.4.4. *Impurities of the Type X_2O_3*

With the exception of the oxides of boron and yttrium, the effect of oxides of this group is not pronounced. The low value assigned to the oxide of yttrium appears to be unduly influenced by a single experimental point, and one could well expect a value as high as 0.3 from Johnson's Fig. 1.

Admixture of 0.5 mole percent of chromium oxide decreased the conductivity at 1100°C, but produced a sharp increase in conductivity at 500°C. Further increase in admixture of this oxide caused little change in conductivity. The apparent activation energy was reduced by a factor of three by the admixture of 0.5 mole percent. This apparent change in activation energy appears to be associated with a different mechanism of conductivity. This conclusion is strengthened by the oxygen pressure dependence of the conductivity of this material, discussed in another section.

[56] S. I. Gorelik, J. Exptl. Theoret. Phys. U.S.S.R. **21**, 826 (1951).

6.4.5. *Impurities of the Type XO_2*

The effect of the oxide of silicon appears to be surprisingly high in view of the valence assumed by this element.

6.4.6. *Impurities of the Types X_2O_5 and XO_3*

Some of the largest effects were produced by oxides in these groups. However, the low values corresponding to the oxides of molybdenum and vanadium are remarkable. The difference between the elements molybdenum (atomic number 42) and niobium (atomic number 41) is interesting, as is the difference between the effect of the oxides of tungsten (atomic number 74) and tantalum (atomic number 73).

Table IV summarizes the effect of adding certain oxides to rutile containing 0.5 mole percent of niobium oxide. The large effect of aluminum oxide is readily explained. The trivalent ion has a noble gas configuration, hence a comparatively large amount of energy is required for the removal of the fourth electron. Aluminum occupies a titanium site in the crystal structure but remains in the trivalent state. The association of trivalent aluminum and pentavalent niobium ions preserves electrical neutrality without the formation of trivalent titanium ions. Hence the large reduction in the electrical conductivity of the niobium-doped rutile resulting from the addition of aluminum oxide.

Unfortunately this explanation does not account for the enormous difference between the effects of the other oxides listed in Table IV. The fourth ionization potentials are believed to lie in the range 50 to 64 ev (compare with that of aluminum: 120 ev).

The effect is not closely related to the ionic radius, since the value for trivalent gallium (0.26 A) is only slightly smaller than the ionic radius of trivalent chromium (0.64 A).

Gallium, indium, and chromium are known to exhibit more than one valence in the formation of oxides. The extreme values in the table are for the oxides of aluminum and yttrium, both of which form only trivalent ions with noble gas configurations. A satisfactory theory of these effects would have to explain the remarkable difference between the effects of these oxides.

6.4.7. *The Results of Hauffe and Co-Workers*

Hauffe[47] and co-workers have found that the admixture of a small amount of WO_3 to rutile increases the conductivity enormously (page 136 of reference 47). The effect is more pronounced at 600°C than at 900°C. These workers have also investigated the effect of admixture of the oxides of nickel, gallium, aluminum, and chromium on the electrical conductivity of rutile ceramic in the range 600 to 900°C. The effect of the oxides of aluminum, nickel, and gallium was small, and produced no apparent change in the activation energy for the impurity range 0 to 2.0 mole percent.

TABLE IV. Effect of 1 mole % of (other) impurity on rutile containing 0.5 mole % Nb_2O_5 ($\sigma = 3\times10^{-4}$ ohm^{-1} cm^{-1}) (after Johnson[a]).

Impurity	Change in conductivity
Al_2O_3	÷35 000
Y_2O_3	÷ 58
Ga_2O_3	÷80 000
In_2O_3	÷ 990
Cr_2O_3	÷ 550

[a] See reference 55.

6.4.8. *Effect of Impurity Concentration*

Johnson attempted to estimate the percentage of foreign oxide that can be taken into solution at 1200°C and retained in this state during subsequent heat treatment, i.e., air-quenching to 250°C. This result showed a saturation effect in most cases at concentration above about 0.25 to 0.50 mole percent.

The conductivity was highly dependent on the heat treatment a sample received, and the rate of cooling determined the degree to which "exsolution" occurred. It would be of interest to establish the extent to which these effects are (a) dependent on the formation of impurity bands and (b) are determined by the solubility of the added oxide in rutile. In case (a) it is probable that there exists a correlation between these results and the paramagnetic susceptibility of these doped specimens.

7. THERMOPOWER

7.1. Introduction

The electrical circuit for the measurement of the thermopower (or Seebeck coefficient) of a semiconductor S with respect to a metal M, is represented schematically in Fig. 6. The junctions are maintained at temperatures T_1 and T_2, where T_2 is greater than T_1. The thermopower of S with respect to M is defined as

$$Q_S - Q_M = -d(V_2 - V_1)/d(T_2 - T_1) \qquad (7\text{-}1)$$

when the net current in the circuit is zero.

Since thermal emf's are additive, it has a meaning to talk of the absolute thermopower of a substance. This is particularly true of semiconductors, since they exhibit much larger thermoelectric effects than metals.

It is shown by Seitz[57] and by Domenicali[58] that the thermopower, Q, consists of the two terms,** and can be represented by

$$Q = (1/e)((\eta - Q^*)/T). \qquad (7\text{-}2)$$

Q^* is the heat transport per electron, which in semiconductors is approximately $2kT$, and so this term

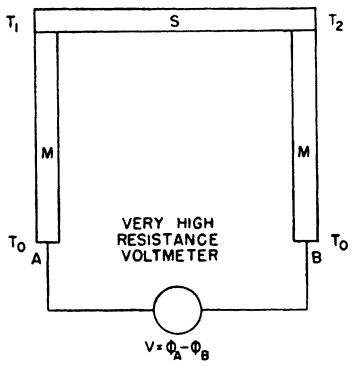

FIG. 6. Circuit for the measurement of the thermopower of a semiconductor S with respect to a metal M, using an electrostatic voltmeter V.

contributes about -170 μv per degree to the thermopower, at all temperatures. The first term on the right-hand side of Eq. (7-2) has the same sign as the Fermi potential of the electrons, η, so that when the Fermi level lies below the bottom of the conduction band this term is negative.

In practice, the small thermopower of the metal is usually neglected in comparison with the much larger value for the semiconductor, so that the measured potential difference is given by the expression

$$F_s = V_1 - V_2 = \int_{T_2}^{T_1} Q_S dT. \qquad (7\text{-}3)$$

The interpretation of Q_S in terms of the choice of band model is discussed in Sec. (5-5).

7.2. Experimental Results

Kataoka and Suzuki[59] have measured the thermopower of ceramic rutile in various stages of reduction. Their high resistivity specimens (3000 ohm cm at 300°K) exhibited a thermopower of -1.03 mv/°C in the range 0 to 90°C. The thermopower, as expected, decreased with increasing impurity content. The specimens of lowest resistivity (0.05 ohm cm at 300°K) exhibited a thermopower of -0.17 mv/°C between 0 and 100°C, falling to about -0.15 mv/°C between 150 and 200°C. Some of their curves of thermopower *versus* temperature were concave toward the temperature axis.

These workers claim to have established a correlation between thermopower and the conductivity of the specimens. The difficulties encountered in making such a correlation due to the uncertainty in the values of the mobility, the effective mass, and in the dynamic term Q^*/eT of the thermopower are discussed in Sec. (5.5.2).

However, the thermopower may be plotted against reciprocal temperature to yield a value for the ioni-

[57] Frederick Seitz, *The Modern Theory of Solids* (McGraw-Hill Book Company, Inc., New York, 1940).

[58] C. A. Domenicali, Revs. Modern Phys. **26**, 237 (1954).

** It is assumed that these transport phenomena are determined entirely by the electronic mobility, and not by that of holes.

[59] S. Katoaka and T. Suzuki, Bull. Electrotech. Lab. Tokyo **18**, No. 1, 732 (1954).

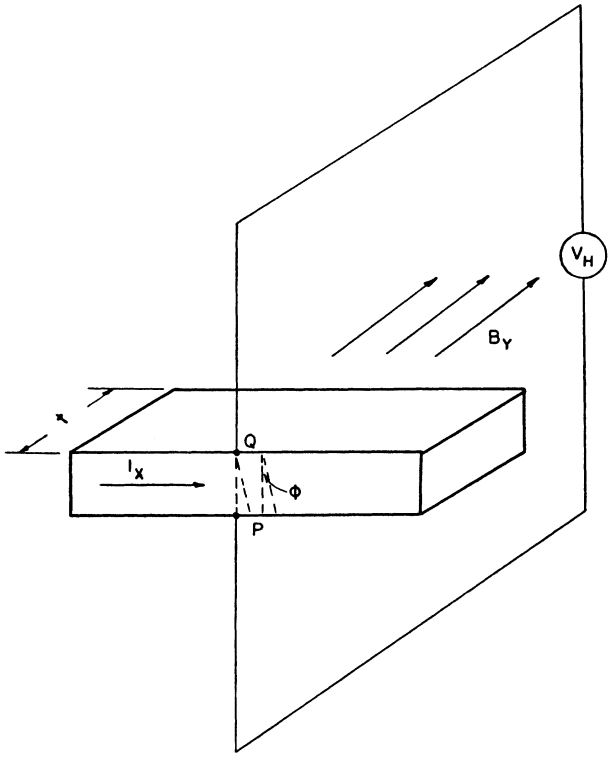

FIG. 7. Schematic diagram of apparatus for Hall effect measurements.

zation potential of the donor sites, to the extent that the simple band model used in deriving Eq. (5-23) is valid. This procedure, applied to the data on page 735 of reference 59 yields values of E_d (noninteracting donor model) in the range -0.02 to -0.13 ev. There appears to be no correlation between the values obtained in this way and those obtained from conductivity data, discussed in Sec. (6.3.1).

When the values of the Fermi level (donor band model) are obtained from these same data by the use of Eq. (5-24), one obtains values ranging from -0.31 ev to zero, the position of the Fermi level rising with increasing donor concentration (as evidenced by the resistivity measurements).

These workers have also shown that the thermopower of their specimens is dependent on the ambient atmosphere. At a pressure of 10^{-1} of mercury the thermopower of their specimens was more highly temperature dependent than at atmospheric pressure.

Boltaks and co-workers[60] have investigated the thermopower Q of sintered rutile that had been reduced in hydrogen or in carbon monoxide. In all cases the thermal emf was negative. Here, Q was found to decrease with increased reduction. The experimental values lay in the range -250 to -415 μv per degree. Thus, Q decreased with increasing temperature for the slightly reduced samples. The thermopower of the highly reduced samples, however, increased with increasing temperature. This latter effect may have resulted from partial reoxidation.

[60] Boltaks, Vasenin, and Salunina, Zhur. Tekh. Fiz. **21**, 532 (1951).

8. THE HALL EFFECT

The Hall effect arises from the force experienced by a charge moving in a magnetic field. A high resistance voltmeter is connected to the electrodes P and Q on the lower and upper faces (Fig. 7) of the specimen of uniform rectangular cross section, and thickness t cm, in which a current I_x amp is flowing. The electrodes P and Q are assumed to be placed so that they are at the same potential before the application of a magnetic field. When a magnetic field B_y gauss is applied in a direction normal to the current I_x and parallel to the t direction, a potential difference $V_H(=V_Q-V_P)$ volts appears between the electrodes. The quantity $R=10^8V_Ht/B_yI_x$ is defined as the Hall coefficient. When lattice scattering predominates, the concentration of charge carriers n is related to the Hall coefficient by the formula

$$n=-7.40\times10^{18}G/R. \tag{8-1}$$

For n-type semiconductors, G is a function of the Fermi level which varies between 1 for nondegenerate samples, to $8/3\pi$ for completely degenerate samples.[61,62] When impurity scattering cannot be neglected, this value of n must be corrected[63] by a factor r, which has a value in the range 1 to 2 for ionized impurity scattering.

8.1. Hall Data of Reduced Rutile

Breckenridge and Hosler[61] have made Hall measurements on samples of rutile ceramic and single crystals which had been subjected to various degrees of reduction in hydrogen. These workers then attempted to interpret the values of the electron concentration n obtained by the use of Eq. (8-1) in terms of two sources of conduction electrons, one of which has a very small activation energy, so that it was considerably ionized even at liquid air temperature. Their results (Fig. 8) were interpreted in terms of the following equation

$$n=n_1\exp(\Delta E_1/2kT)+n_2\exp(\Delta E_2/2kT) \tag{8-2}$$

with $\Delta E_1\ll\Delta E_2$, and $n_1\ll n_2$.

Interpretation of ΔE_1 and ΔE_2 in terms of the ionization potentials of isolated donor type impurities is complicated by the effect of the $\frac{3}{4}\ln t$ correction term of Eq. (5-6). This correction is important even for ΔE_2, whereas the significance of the smaller ΔE_1 is almost entirely lost because of the magnitude of the correction term.

[61] R. G. Breckenridge and W. R. Hosler, Phys. Rev. **91**, 793 (1953).

[62] K. Shifrin, J. Phys. (U.S.S.R.) **8**, 242 (1944).

[63] W. Crawford Dunlap, Jr., *An Introduction to Semiconductors* (John Wiley & Sons, Inc., New York, 1957); see Fig. 6.5.

Attempts have been made below to interpret the Hall data of Breckenridge and Hosler[61] under the assumption that the form of the curves at higher temperatures (200 to 500°K) is determined by the electrons in the conduction band, to which Maxwell-Boltzmann statistics and the concept of a single effective electron mass are assumed to apply. In the first case, the source of these electrons is considered to be non-interacting donor sites at an energy E_d with respect to the bottom of the conduction band. The appropriate type of plot for the experimental data is suggested by Eq. (5-6), and from the slope a value of E_d may be obtained.

In the second case, the appropriate type of plot is indicated by Eq. (5-7), in which no assumption concerning the source of electrons is implied. However, the slope of the plot yields the height of the Fermi level, which will lie near the center of the donor band if it exists. In this case the plot yields also the effective mass of the conduction electrons.

At the temperatures considered, the effect of the magnetic field on the concentration of conduction-band electrons is believed to be entirely negligible.[64]

When the data of Breckenridge and Hosler's Fig. 11 are plotted in these two different ways for the temperature range 250 to 500°K, the results are as follows. With the exception of one very low value, for curve (*b*), the values of E_d (noninteracting donors) lie in the range -0.095 to -0.147 ev. With the same exception, the values of the Fermi level (donor band model) lie in the range -0.025 to -0.051 ev with respect to the bottom of the conduction band. The corresponding values of the effective mass ratio are in the range 0.16 to 1.6. Although Maxwell-Boltzmann statistics can scarcely be said to apply to these data, these values of the effective mass of the conduction electrons are much lower than the values usually quoted for rutile.

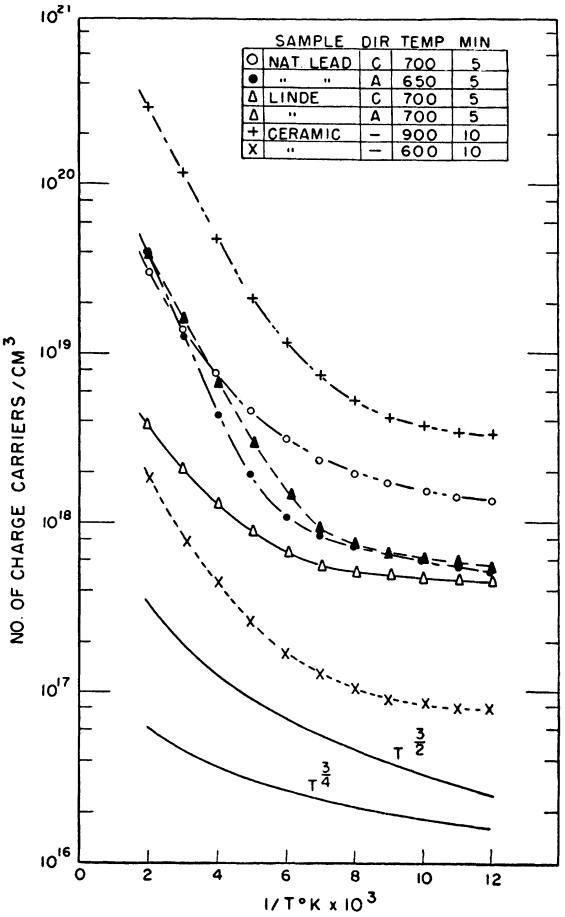

FIG. 8. Electron concentrations in specimens of rutile reduced in hydrogen under the conditions specified (after Breckenridge and Hosler[61]). Curves showing the temperature variation of the factors $T^{3/4}$ and $T^{3/2}$ of Eqs. (5-5) and (5-7) are shown for comparison.

8.2. Hall Mobility

An electric charge moving in the x direction normal to a magnetic field B_y, "sees," in addition, an electric field E_z, where

$$E_z = v_x B_y \quad \text{(mks units)}.$$

Since the mobility b is defined as v_x/E_x, we obtain

$$E_z/E_x = b_H B_y \quad \text{(mks units)}.$$

Hence the equipotential surfaces in a conductor are rotated by the magnetic field through an angle ϕ, where $\tan\phi = b_H B_y$. In cgs units

$$\tan\phi = 10^{-8} b_H B_y.$$

This simple relation is somewhat obscured by the usual derivation of the Hall mobility from the electrical conductivity and the Hall coefficient

$$\sigma = neb$$
$$-R = 1/ne$$
$$(-R\sigma) = b_H. \tag{8-3}$$

The determination of b_H from simultaneous measurements of σ and R is entirely equivalent experimentally to the measurement of $\tan\phi$, so that the simple interpretation of the Hall mobility is unaltered.

Figure 9 illustrates a typical Hall mobility curve derived from the electrical conductivity and Hall data of Breckenridge and Hosler. These workers attempted to interpret their results in terms of the theory of scattering by optical lattice vibrations developed by Fröhlich and Mott,[65] and by Fröhlich, Pelzer, and Zineau.[66] The additional scattering at low temperatures

[64] P. T. Landsberg, Proc. Phys. Soc. (London) **71**, 69 (1958).

[65] H. Fröhlich and N. F. Mott, Proc. Roy. Soc. (London) **A171**, 496 (1939).

[66] Fröhlich, Pelzer, and Zineau, Phil. Mag. **41**, 221 (1950).

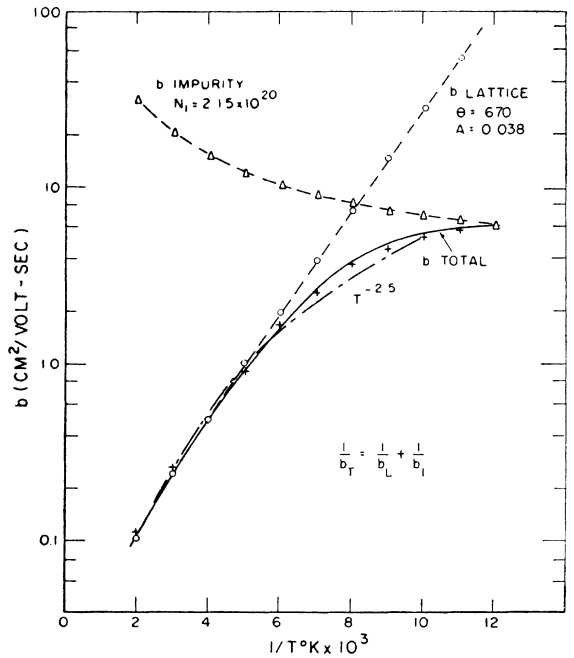

FIG. 9. Hall mobility in a sample of reduced rutile, after Breckenridge and Hosler.[61] The dotted curve, showing a $T^{-2.5}$ dependence, is included for comparison. The symbols and A refer to the constants in Eq. (5-13).

was ascribed to the effect of impurities as treated by Conwell and Weisskopf.[67]

When an empirical relation for the temperature dependence of the mobility is required to assist in the interpretation of conductivity data above about 200°K, a $T^{-2.5}$ law appears to be satisfactory. For comparison purposes, a $T^{-2.5}$ plot is included in Fig. 9.

8.3. Magnetoresistance

Gorelik[68] has investigated the effect of a magnetic field of 15 000 gauss on the electrical conductivity of "pure" rutile, and on specimens of rutile containing various proportions of the oxides of calcium and strontium. The entire change in conductivity did not occur immediately after the application of the magnetic field, but was practically complete after two minutes. The change in conductivity was small at room temperatures, but above about 160°C the fractional change in conductivity rose to steady values of one or two percent.

Gorelik has given an "explanation" of these effects in terms of the relative importance of the ionic and electronic contributions to the conductivity.

9. MAGNETIC SUSCEPTIBILITY

9.1. Introduction

In a semiconductor, such as rutile, one must consider the following four contributions to the magnetic susceptibility[69]: (a) the lattice susceptibility, (b) the carrier susceptibility, (c) the contribution of the impurities, including effect of departures from stoichiometry. This effect may be differentiated into two cases (i) the effect of noninteracting sites, and (ii) the effect of donor (or acceptor) bands; and (d) the effect of surface states, including adsorbed gases.

9.2.(a) Lattice Susceptibility

Van Vleck[70] gives the following expression for the lattice susceptibility, and points out that there is no sharp dividing line between diamagnetic molecules and feebly paramagnetic ones:

$$\chi_{\text{mole}}=-\frac{Le^2}{6mc^2}\sum\langle r^2\rangle+\tfrac{2}{3}L\sum_{n'\neq n}\frac{|m^0(n';n)|^2}{h\nu(n';n)}. \quad (9\text{-}1)$$

In Eq. (9-1), $m^0(n';n)$ is a nondiagonal element of the vector matrix for the magnetic moment of the system, evaluated in the absence of a field, $\nu(n';n)$ is the frequency corresponding to the $n';n$ transition. L is Avogadro's number, e the electronic charge in esu, m the electronic mass in grams, and c is the speed of light in cm/sec. $\sum\langle r^2\rangle$ is the mean value of the radius of an electron orbit, summed over all the electrons.

When the second term of Eq. (9-1) predominates, the contribution represents a small, almost temperature-independent paramagnetism. Using the simple ionic model, the ions in the oxides Sc_2O_3, TiO_2, V_2O_5, and CeO_2 possess noble gas configurations, hence would be expected to have a negative (diamagnetic) lattice susceptibility. However, there appears to be some evidence, especially in the case of V_2O_5, for a contribution due to temperature-independent paramagnetism larger than the negative (diamagnetic) term.[71–74] Freed and Kasper[75] discuss this effect in ions of the type VO_2^{+2}, WO_4^{-2}, MnO_4^{-}, VO_3^{-}, and $Cr_2O_7^{-2}$. Bates[76] considers that the feeble paramagnetism believed to exist in Sc_2O_3, TiO_2, and CeO_2 may be caused by the "distortion due to interatomic forces," and adds that it is difficult to determine in a given case whether the effect is due to a negative exchange integral, to electron migration (in conductors), or to ionic deformation.

At least in the case of rutile, the wide range of experimental values reported in the literature, which include both positive and negative values, may result from departures from stoichiometry. The formation of oxygen vacancies (and Ti^{+3} sites) which result when

[67] E. Conwell and V. F. Weisskopf, Phys. Rev. **77**, 388 (1950).
[68] S. I. Gorelik, J. Exptl. Theoret. Phys. **21**, 826 (1951).
[69] Stevens, Cleland, Crawford, and Schweinler, Phys. Rev. **100**, 1084 (1955).
[70] J. H. Van Vleck, *The Theory of Electric and Magnetic Susceptibilities* (Oxford University Press, New York, 1932), pp. 275, 279, 302–303.
[71] T. Ishiwara, Sci. Rept. Tôhoku Univ. **3**, 303 (1914).
[72] P. Weiss and P. Collet, Compt. rend. **178**, 2146 (1924); **181**, 1057 (1925).
[73] R. Ladenburg, Z. physik. Chem. **126**, 133 (1927).
[74] L. F. Bates, *Modern Magnetism* (Cambridge University Press, New York, 1951), pp. 272, 44.
[75] S. Freed and C. Kasper, J. Am. Chem. Soc. **52**, 4671 (1930).
[76] Reference 74, pp. 281 and 324.

rutile is prepared at moderately high temperatures in a reducing atmosphere is discussed in Sec. 14. The various values of the magnetic susceptibility of "pure, stoichiometric" rutile, appearing in the literature, are listed in Table V.

9.3.(b) Carrier Susceptibility

Assuming that the carrier electrons behave as a perfect electron gas, and using the appropriate density-of-states effective mass ratio, the following expression for the carrier susceptibility has been derived[69,77]:

$$\chi_c=\left(\frac{\beta^2}{3kT}\right)n_c[3-\langle f_e^2\rangle_{Av}], \tag{9-2}$$

where n_c is the concentration of electrons in the conduction band, β is the Bohr magneton, and $\langle f_e^2\rangle_{Av}$ depends on the curvature of the energy surfaces in k space. This term is related to the effective mass ratio for orbital motion M^M by the relation

$$M^M=(\langle f_e^2\rangle_{Av})^{-\frac{1}{2}}. \tag{9-3}$$

Since M^M is expected to be considerably larger than unity in the case of rutile,[78] Eq. (9-2) may be approximated by the relation

$$\chi_c=\beta^2 n_c/kT, \tag{9-4}$$

which is of the same form as the contribution of unpaired electrons in noninteracting hydrogen-like donors to be discussed in the next paragraph.

9.4.(c) Impurity Contribution

Mooser[79] has discussed (i) the contribution of electrons in noninteracting hydrogen-like impurity sites, and (ii) the case in which the overlapping of the impurity wave functions is sufficiently great for the formation of impurity bands. Considering first the case in which the donor sites are noninteracting and are in s-like ground states, he obtains

$$\chi_{\text{para}}=n_d\beta^2/kT, \tag{9-5}$$

where n_d is the concentration of occupied donors, which is related to N_d, the concentration of donor sites, by the following relation:

$$n_d=N_d/1+\tfrac{1}{2}\exp((E_d-\eta)/kT). \tag{9-6}$$

Here, $E_d-\eta$ is the energy of the donor levels with respect to the Fermi level η.

A diamagnetic term must be added to Eq. (9-5) so that the total contribution of the electrons in isolated, hydrogen-like donor sites is given by the following expression:

$$\chi=n_d(\beta^2/kT-e^2r^2/6m_ec^2) \tag{9-7}$$

in which r is the radius of the electron orbit in cm, e is the electronic charge in esu, c is the velocity of light in cm sec^{-1}, and m_e is the effective mass of the electrons in grams.

If the assumption of a high effective mass M^M, implied in Eq. (9-4) is valid, comparison of this relation with the expression for the paramagnetic contribution of (atomic) hydrogen-like donors shows that they are of the same form. In this case, the paramagnetic susceptibility is independent of the distribution of the unpaired electrons between the donor sites and the conduction band, i.e., the thermal ionization of donor sites does not affect their contribution to the susceptibility. This is in contrast to the case in which the wave functions of the impurity sites overlap sufficiently for the formation of impurity bands. This point is discussed later.

TABLE V. Magnetic susceptibility of rutile.

Source	Temperature	Magnetic susceptibility (emu per gram)
Meyer[a]	288°K	0.37×10^{-6}
Wedekind and Hausknecht[b]	room	0.066
Berkman and Zocher[c]	room	−0.20
Hüttig[d]	room	−0.30
Raychaudhuri and Sengupta[e]		0.073
Ehrlich[f]	90 and 293°K	0.08
Zimens and Hedvall[g]		0.134
Hill and Selwood[h]	i	−0.3
Reyerson and Honig[j]	301°K	0.061[k]

[a] S. Meyer, Ann. Physik **69**, 236 (1899).
[b] E. Wedekind and P. Hausknecht, Ber. deut. chem. Ges. **46**, 3763 (1913).
[c] S. Berkman and H. Zocher, Z. physik. Chem. **124**, 322 (1926).
[d] G. F. Hüttig, Z. anorg. u. allgem. Chem. **224**, 225 (1935).
[e] D. P. Raychaudhuri and P. N. Sengupta, Indian J. Phys. **10**, 253 (1936).
[f] See reference 80.
[g] K. Zimens and J. Hedvall, Svensk Kem. Tidsk. **52**, 12 (1941).
[h] F. N. Hill and P. W. Selwood, J. Am. Chem. Soc. **71**, 2522 (1949).
[i] "Substantially independent of temperature," presumably down to −190°C.
[j] L. H. Reyerson and J. M. Honig, J. Am. Chem. Soc. **75**, 3920 (1953).
[k] See discussion of adsorption of NO_2-N_2O_4 on rutile.

9.4.1. *Electrons in Impurity Bands*

The diamagnetic contribution of electrons in impurity bands is believed to be small and about the same as that of electrons in noninteracting donor sites [the second term in Eq. (9-7)].

Band wide compared with kT.—At low temperatures the paramagnetic contribution is given by the following expression

$$\chi_{\text{para}}=2\beta^2D(\eta) \tag{9-8}$$

in which $D(\eta)$ denotes the density of states in the donor band at the position of the Fermi level. In this temperature range χ should be almost independent of temperature.

Band narrow compared with kT.—At high temperatures, where the band width is much less than kT, the paramagnetic contribution of the electrons in the

[77] H. Fröhlich, *Theorie der Metalle* (Verlag Julius Springer, Berlin, 1937), pp. 144–156.
[78] R. G. Breckenridge and W. R. Hosler, Phys. Rev. **91**, 793 (1953).
[79] E. Mooser, Phys. Rev. **100**, 1589 (1955); G. Busch and E. Mooser, Helv. Phys. Acta **24**, 329 (1951); **26**, 611 (1953); Z. physik. Chem. **198**, 23 (1951).

TABLE VI. Fraction of donor electrons contributing to magnetic susceptibility of TiO_x (after Ehrlich).

x	Temperature °K	O_v Oxygen vacancies per mole of TiO_2	n_D Donor electrons per mole of TiO_2 (2 per O_v)	Experimental χ_{para} per mole[a]	n_D' (calculated from χ_{para}) donor electrons per mole	$f=\frac{n_D'}{n_D}$
1.97	293	1.8×10^{22}	3.6×10^{22}	46×10^{-6}	2.2×10^{22}	0.61
1.95	293	3.0	6.0	72	3.5	0.57
1.90	293	6.0	12.0	119	5.7	0.47
1.97	90	1.8	3.6	104	1.54	0.42
1.95	90	3.0	6.0	162	2.39	0.40
1.90	90	6.0	12.0	216	3.19	0.26

[a] After correction for temperature-independent paramagnetic lattice susceptibility ($+6\times10^{-6}$ emu per mole).

impurity band is obtained from the result obtained for the noninteracting donor sites by multiplying by the factor f, which indicates the fraction of the electron spins that are "free" (see Sec. 9.4.2)

$$f=\exp((\bar{E}_d-\eta)/kT)/(1+\exp(\bar{E}_d-\eta)kT), \quad (9\text{-}9)$$

where $\bar{E}_d$ is the energy of the midpoint of the donor band. This factor has the value unity when the Fermi level lies far below the donor band. In the case of principal interest $(\bar{E}_d-\eta)$ is zero or slightly negative, and the multiplying factor is approximately equal to $\frac{1}{2}$. When the Fermi level is more than $3kT$ higher than the donor band f is very small, tending to zero with increased separation.

The numerical value of this factor is therefore highly dependent on the height of the Fermi level. The dependence of the Fermi level on temperature has been discussed in Sec. 5.

Once again it is necessary to draw attention to the high dielectric constant in rutile. It is therefore probable that impurity bands form at lower impurity concentrations than in most other materials. This effect may be offset by the possibly high effective electron mass.

9.4.2. Donor Sites in Nonstoichiometric Rutile

Although the contribution of the Ti^{+4} ions to the magnetic susceptibility is small, and of uncertain sign, the Ti^{+3} ion definitely makes a large contribution to the paramagnetic susceptibility of the crystal. Departures from stoichiometry of rutile are believed to result in the conversion of Ti^{+4} sites to Ti^{+3} sites. These ions of lower valence may in many ways be considered to constitute an "impurity" in the rutile lattice, and in this section the terms "impurity site" and "impurity band" are understood to apply to nonstoichiometric rutile.

Ehrlich[80] has investigated the magnetic susceptibility of solids of the composition TiO_x from $x=0$ to $x=2$. If it is assumed that the formation of an oxygen vacancy results in the formation of two Ti^{+3} sites, each with a magnetic moment of 1.73 Bohr magnetons, one may calculate the resulting paramagnetic susceptibility. For example, Ehrlich estimated that the paramagnetic susceptibility of rutile which had been reduced to the extent of two percent weight loss ($x=1.90$) should be 253×10^{-6} per gram mole at room temperature. Since the experimental value was 119×10^{-6} he concluded that only 47% of the electrons were "free."

Ehrlich's calculations have been extended to his other data, and are summarized in Table VI. As expected, the fraction f of the donor electrons that contribute to the susceptibility (column 7) decreases with increasing donor concentration.

However, we note the higher values of f for the room temperature measurements as compared with the measurements at 90°K.

Now subject to the assumptions of a high effective mass ratio M^M and the applicability of Maxwell-Boltzmann statistics, the raising of electrons from isolated hydrogen atom-like donors to the conduction band should not appreciably alter the paramagnetic susceptibility. We therefore look for an explanation in terms of overlapping of donor wave functions and the formation of a donor band.

A very approximate value for the width of this hypothetical band may be obtained from Ehrlich's low temperature data by the application of Mooser's expression for the susceptibility of electrons in bands wide in comparison with kT. Here, $\chi=2\beta^2D(\eta)$ where $D(\eta)$ represents the density of states at the Fermi level. The total number of levels was taken to be twice the number of oxygen vacancies. The approximation was introduced that the density of states D was uniform throughout the band, whence ΔE was estimated. The results of calculations for TiO_x (where $x=1.90$, 1.95, and 1.97) at 90°K appear in Table VII. The estimated values of ΔE are somewhat larger than kT (which is 0.0077 eV at 90°K), so that the requirement regarding the width of the band is fulfilled.

It is now necessary to account for the observed increase in f with increasing temperature. One may ask whether this increase could reflect a transition from the "wide band" case, at 90°K, to the "narrow band" case. The estimated band widths (last column of Table VII) are about fifty percent greater than kT at 293°K. It is not unreasonable to suppose that the 293° values represent an intermediate case, and that at still higher

[80] P. Ehrlich, Z. Electrochem. **45**, 362 (1939).

temperatures the "narrow band" approximation would be valid. Earlier, it was concluded that the Fermi level would be expected to lie at, or somewhat lower than, the middle of the donor band. In the "narrow band" limit, the expected value of f calculated from Eq. (9-8) is therefore equal to, or greater than, $\frac{1}{2}$. The observed values of f (given in the last column of Table VI) appear to be consistent with this interpretation.

An alternative explanation may be given if two electrons are bound to each oxygen vacancy at sufficiently low temperatures, and these sites are assumed to be noninteracting. One would expect the electron spins to be paired in such a "molecule." Raising of one or both of these electrons to higher states by thermal excitation would uncouple the spins. This conclusion is valid, regardless of the extent of the overlapping of the wave functions of the higher states, provided that the Fermi level lies farther than about $3kT$ below the bottom of any such higher band [see Eq. (9-9)]. If the Fermi level lay closer to this higher band than about $3kT$, the Pauli principle, would have to be invoked, and the value of f would remain below unity.

Ehrlich's results may also be expressed in terms of the Curie-Weiss law (discussed further in the next section), in which case one obtains an effective magnetic moment of 1.5 Bohr magnetons, instead of the expected value of 1.73, and Weiss constants of 700, 72, and 160°K, respectively, for the three compositions $x=1.97$, 1.95, and 1.90.

Gray[81] has reported an investigation of the magnetic susceptibility of "titanium dioxide" during reduction by hydrogen. Simultaneous measurements were made of the decrease in hydrogen pressure, sample weight loss, and paramagnetic susceptibility increase, the temperature being maintained at 560°C. There appears to be an almost linear relation between change in susceptibility and the loss in weight. The sample weight and the method of measurement were not stated and without this information a satisfactory interpretation of the data cannot be made.

9.4.3. *Rutile Containing Impurities*

Representation of the paramagnetic susceptibility arising from donor sites in solids is not often made in terms of the foregoing model invoking donor bands. More commonly the departures from the Curie law are represented empirically by replacement of the T factor in this law by the factor $(T-\Delta)$. This procedure is quite empirical, and may include the effects resulting from the "pairing" of electrons, and the formation of donor bands, discussed in the foregoing.[82,83] Most of the published experimental results are expressed in terms of the magnetic moment of the unpaired electron and the corresponding Weiss constant Δ.

TABLE VII. Width of hypothetical impurity band in TiO_x estimated from Ehrlich's 90°K magnetic susceptibility data.

x	χ_{para} per mole[a]	Number of states per mole (2 per O_v)	Calculated density of states at Fermi level $D(\eta)$ per ev	ΔE estimated width of donor band ev
1.97	104×10^{-6}	3.6×10^{22}	99×10^{22}	0.036
1.95	162	6.0	154	0.039
1.90	216	12.0	206	0.058

[a] After correction for temperature-independent paramagnetic lattice susceptibility ($+6\times10^{-6}$ emu per mole).

Selwood[84] and co-workers have shown the "pure" titanium sesquioxide to be antiferromagnetic, with a critical point near the specific heat anomaly at about 248°K. The Weiss constant was unusually large, and was estimated to be about 2000°K. The corresponding magnetic moment for the Ti^{+3} ion was 1.2 Bohr magnetons, which may be compared with the expected value of 1.73 for the free Ti^{+3} ion with one unpaired electron. These results are contradicted by the later work of Foëx and Wucher,[85] and of Pearson.[86] These workers found a continuous increase in susceptibility as the temperature was increased from −200 to about 360°C, the temperature dependence being most pronounced in the vicinity of 160°C.

When paramagnetic ions are separated by solution in a suitable diamagnetic crystal, their mutual interaction is reduced. An example of this effect appears in the work of Adler and Selwood,[87,88] who have studied a solid solution of 14.3% Ti_2O_3 in the diamagnetic oxide, Al_2O_3. The Ti^{3+} ion was found to have a magnetic moment of 1.1 Bohr magnetons (expected value $\sqrt{3}$ Bohr magnetons), and a value of $\Delta=105$°K was obtained. This value of the Weiss constant Δ may be compared with the value of about 2000° obtained for undiluted Ti_2O_3.

Selwood and co-workers have investigated the incorporation of ions of other transition metals into the rutile crystal lattice. The Weiss constant of the manganese ion tends to zero as expected at infinite dilution, and is almost proportional to the concentration.[89] At a concentration of 19% manganese by weight, Δ is about 315°. The magnetic moment corresponds to a valence state of about 4.1 at zero concentration, falling to

[81] T. J. Gray, *The Defect Solid State* (Interscience Publishers, Inc., New York), p. 287.

[82] Other factors affecting the Weiss constant: the multiplet separations and the effect of inhomogeneous electric crystalline fields are discussed on page 150 of reference 84.

[83] R. K. Wangness has discussed the relation between the exchange coupling between spins, and the Curie-Weiss law. R. K. Wangness, J. Chem. Phys. **20**, 1656 (1952).

[84] Pierce W. Selwood, *Magnetochemistry* (Interscience Publishers, Inc., New York, 1956), p. 329.

[85] M. Foëx and J. Wucher, Compt. rend. **241**, 184 (1955).

[86] A. D. Pearson, Technical Report 120, Laboratory for Insulation Research, Massachusetts Institute of Technology, (1957).

[87] Reference 84, p. 161.

[88] S. F. Adler and P. W. Selwood, J. Am. Chem. Soc. **76**, 346 (1954).

[89] Selwood, Moore, Ellis, and Wethington, J. Am. Chem. Soc. **71**, 693 (1949).

about 3.9 as the concentration is increased to 19% manganese (by weight).

The valence state of nickel incorporated into the rutile lattice decreases somewhat with increasing concentration.[90] Extrapolation back from the lowest concentration appearing in the curves (about four percent nickel by weight) indicates that the magnetic moment at infinite dilution is probably between 3.8 and 4.0, considerably lower than expected for six (or four unpaired) electrons. However, from the color, and for other reasons, Selwood believes that the oxidation state is indeed +4.

Similar results were obtained for chromium[91] and iron[92] incorporated into the rutile lattice. In the case of iron, Δ fell from 52° at 12.9% iron, to 16° at 1.5% iron (by weight). The corresponding values of the oxidation state were 3.2 and 3.9. The chromium ion in rutile (2.6% by weight) exhibited a magnetic moment of 2.8 Bohr magnetons, and a negative Δ (−27°).

Thus with the possible exception of nickel, these elements assume a valence state of almost four when occupying titanium sites (at sufficient dilution). Selwood has applied the term "induced valence" to this phenomenon.

9.5.(d) Surface Contribution

The magnetic susceptibility will include the contribution of adsorbed gases, in particular physically adsorbed oxygen. The meaning of the term chemisorption when applied to oxygen and metallic oxides is not clear. However, the nature of the space-charge-barrier layer at the surface of a semiconductor (of the order of 10^{-5} cm thick) is influenced by the chemisorption of gases. Any factor which influences the height of the Fermi level in this region will alter the paramagnetic susceptibility. The importance of this effect is expected to increase as the particle size is reduced.

Sandler[93] has used the rate of *ortho-para* conversion of hydrogen on rutile powder as an indication of the surface density of unpaired electrons arising from the paramagnetism due to surface defects. These defects are believed to be due to a stoichiometric deficiency of oxygen. This surface paramagnetism is apparently associated with the blue color of reduced rutile.

A mention of the investigation of the surface paramagnetism of rutile conducted by Reyerson and Honig, and of the effect of reoxidation by NO_2-N_2O_4 will be found in Sec. 12.

[90] F. N. Hill and P. W. Selwood, J. Am. Chem. Soc. **71**, 2522 (1949).
[91] P. W. Selwood and L. Lyon, Discussions Faraday Soc. **8**, 222 (1950).
[92] Selwood, Ellis, and Wethington, J. Am. Chem. Soc. **71**, 2181 (1949).
[93] Y. L. Sandler, J. Phys. Chem. **58**, 54 (1954).

10. THERMAL CONDUCTIVITY, SPECIFIC HEAT, AND VARIOUS PHYSICAL PROPERTIES

10.1. Thermal Conductivity

Kingery and McQuarrie[94] have determined the thermal conductivity of a number of pure ceramic oxides, including rutile, in the temperature range 100 to 1800°C. The results were corrected for the porosity of the samples. Values of 0.0119 and 0.0081 (cal sec^{-1} cm^{-2}) (°C cm^{-1}) at 200 and 800°C, respectively, were obtained. Kingery[95] has discussed the variations in thermal conductivity associated with the effect of radiant energy transmission, the ratio of the phonon mean free path to lattice dimension, the value of the Debye temperature, emissivity, and the relation of the electronic conductivity to the thermal conductivity of rutile.

The thermal conductivities of sapphire and rutile single crystals have been measured in the temperature range −50 to 100°C by McCarthy *et al.*[96] The thermal conductivity is greater parallel to the optic axis than in the direction perpendicular to it. Both values decrease with increasing temperature in the temperature range studied, and their ratio is also temperature dependent.

10.2. Thermal Coefficient of Expansion

Day[97] has obtained a value of 80×10^{-7} per °C, for the coefficient of expansion of rutile in the range −130 to 50°C. Mauer and Bolz[98] have determined the thermal expansion coefficient of stoichiometric and reduced rutile from x-ray data. In the temperature range 0 to 200°C the average values of the coefficient of expansion of stoichiometric rutile were 8.0×10^{-6} in the *a* direction and 9.2×10^{-6} per °C in the *c* direction. In the temperature range 0 to 1000°C the corresponding average values are 8.4×10^{-6} and 9.2×10^{-6} per °C. In the temperature range 0 to 400°C, the average values for reduced rutile ($TiO_{1.97}$) were 8.4×10^{-6} per °C for the *a* direction, and 10.5×10^{-6} per °C for the *c* direction.

10.3. Specific Heat and Debye Temperature

At sufficiently low temperatures, only the low-frequency vibrations are important in determining the internal energy of a solid. In this region the specific heat capacity is expected to be proportional to T^3, and one expects a constant value for the Debye temperature θ. In rutile, this range extends to above 4°K, and Keesom and Pearlman[99] obtained a value of 758°K for the corresponding Debye temperature. In the

[94] W. D. Kingery and M. McQuarrie, J. Am. Ceram. Soc. **37**, 107 (1954).
[95] W. D. Kingery, J. Am. Ceram. Soc. **38**, 251 (1955).
[96] McCarthy, Ballard, and Doerner, Phys. Rev. **88**, 153A (1952).
[97] Jean Day, Bull. soc. sci. Bretagne **24**, 13 (1949).
[98] Floyd A. Mauer and Leonard H. Bolz, National Bureau of Standards, Wright Air Development Center Technical Rept. 55-473 (1955).
[99] P. H. Keesom and N. Pearlman, Phys. Rev. **98**, 1539A (1955).

temperature range 10 to 20°K they found that θ decreases from 650 to 460°K.

Also from specific heat studies, McDonald and Seltz[100] obtained a value of $\theta=670$°K in the temperature range 68 to 298°K.

Basing their calculations on earlier measurements of infrared absorption bands, Breckenridge and Hosler[101] obtained values of $\theta=936$°K and $\theta=1161$°K. However, their interpretation of their Hall mobility data was more consistent with McDonald and Seltz's value of $\theta=670$°K.

After slight reduction in H_2 or Ar, at 1000°C, the heat capacity in the helium region increases greatly.[99] As a tentative explanation, the authors suggested that the additional heat capacity was possibly due to the contribution of the "free" classical electrons. In which band these "free" electrons are to be found, is an open question. From the estimated degeneracy temperature these workers obtained a carrier mass of 350 times the free electron mass.

The heat capacity of rutile powder has been measured in the low temperature region by Shomate.[102] Arthur[103] has made measurements in the range 293 to 1073°K and Naylor[104] in the range 500 to 1800°K. For the heat capacity in calories per mole, valid in the range 500 to 1800°K, Naylor gives the formula:

$$c_p=0.2145+12.3\times10^{-6}T-4380/T^2.$$

Arthur expresses his results in the form

$$c_p=0.1512+0.000245T-0.222\times10^{-7}T^2$$

calories per gram per degree, plus or minus two percent, valid in the range 293 to 1073°K. For purpose of comparison, these formulas yield, respectively, values of 0.217 and 0.333 cal/g/deg, at 800°K.

Dugdale *et al.*[105] expected to find a particle-size effect at low temperatures. Instead, however, they found that the specific heat of rutile was independent of particle size below 50°K. Above this temperature the observed dependence was attributed qualitatively as an effect of the *optical* modes of vibration. Because of the relatively complicated crystal structure of rutile, no attempt was made to make a theoretical calculation of the magnitude of the effect. These workers obtained a value of $C_p=0.115$ cal/mole°K at 20°K and 1.407 cal/mole°K at 50°K.

[100] H. J. McDonald and H. Seltz, J. Am. Chem. Soc. **61**, 2405 (1939).
[101] R. G. Breckenridge and W. R. Hosler, Phys. Rev. **91**, 793 (1953).
[102] C. H. Shomate, J. Am. Chem. Soc. **69**, 218 (1947).
[103] J. S. Arthur, J. Appl. Phys. **21**, 732 (1950).
[104] B. F. Naylor, J. Am. Chem. Soc. **68**, 1077 (1946).
[105] Dugdale, Morrison, and Patterson, Proc. Roy. Soc. (London) **A224**, 228 (1954).

10.4. Miscellaneous Physical Properties

10.4.1. Density

The density of rutile,[106] calculated from x-ray data is 4.28; the pycnometer density is 4.22 g/cc.[107]

10.4.2. Melting Point

St. Pierre[108] has determined the melting point to be 1840±10°C.

10.4.3. Compressibility

The compressibility of natural rutile single-crystals has been investigated by Bridgman.[109] His results could be expressed up to $p=12\,000$ kg/cm^2 by the formula

$$\Delta L/L_0=-a_1p+b_1p^2.$$

From 30° to 75°C the value of a_1 for the c direction was found to vary from 1.038 to 1.090×10^{-7}, and in the a direction was found to vary from 1.871 to 1.954×10^{-7}. For all cases investigated, the value of b_1 was 7×10^{-13}.

10.4.4. Hardness

Moore[110] gives a value of 7 to 7½ (Mohs scale) for the hardness of synthetic rutile crystals. This value is slightly higher than that of quartz. Measurements were made on specimens exhibiting various degrees of reduction, but the variation in hardness in these different specimens was about the same as the variation with crystallographic direction.

10.5. Miscellaneous

A list of references for these and other properties of rutile may be found in "Properties of Titanium Compounds and Related Substances," ONR Report ACR-17, October 1956.

11. DIELECTRIC AND OPTICAL PROPERTIES

11.1. Dielectric Constant and Loss Angle

(a) *Stoichiometric rutile.*—The frequency and temperature dependence of the dielectric constant of stoichiometric rutile have been investigated by Eucken and Büchner,[111] Schusterius,[112] Büttner and Engl,[113] Berberich and Bell[114] and by von Hippel and his coworkers.[115] The dielectric constant shows little variation

[106] Skinner *et al.*, "Titanium and its compounds," Herrick L. Johnston Enterprises (1954).
[107] A. Schroeder, Z. Krist. **67**, 485 (1928).
[108] P. D. S. St. Pierre, J. Am. Ceram. Soc. **35**, 188 (1952).
[109] P. W. Bridgman, Am. J. Sci. **15**, 287 (1928).
[110] C. H. Moore, Jr., Trans. Am. Inst. Mining Met. Petrol. Engrs. **184**, 194 (1949).
[111] A. Eucken and A. Büchner, Z. physik. Chem. **27B**, 321 (1934).
[112] C. Schusterius, Z. tech. Phys. **16**, 640 (1935).
[113] H. Büttner and J. Engl. Z. tech. Phys. **18**, 113 (1937).
[114] L. J. Berberich and M. E. Bell, J. Appl. Phys. **11**, 681 (1940).
[115] von Hippel, Breckenridge, Chesley, and Tisza, Ind. Chem. **38**, 1097 (1946).

with frequency until the region of reststrahl vibrations is reached (wavelengths shorter than about 300 μ).

Thus the measurements of Schmidt[116,117] on single crystals, at a frequency of several hundred megacycles per second are the same as the low-frequency values. This worker obtained a value of 173 for the c direction and 89 for the a direction. These results are in agreement with the values calculated from the reflection measurements of Liebisch and Rubens.[118] The value for densely fired ceramics[115] is approximately 100. If care is taken to prevent the loss of oxygen during firing of the ceramic, the dielectric loss is very low; $\tan\delta = 0.0003$ at 1000 cy/sec and 24°C.

At a frequency of 1000 kcps, the measurements of Bunting *et al.*[119] yielded a value of 106 for the dielectric constant of pure rutile ceramic at −60°C and a value of 93 at 85°C. From these results one obtains a value of -11×10^{-4} for the temperature coefficient of the dielectric constant at 85°C and a value of -7.5×10^{-4} at −60°C.

11.2. Static Dielectric Constant and Polarizability

It is usually assumed that the local field F, effective in polarizing ions in certain types of *diagonal cubic* crystals, is given by the relation

$$F_i = E + \gamma_i P/\epsilon_0 \quad \text{(in mks units)}. \tag{11-1}$$

Following Lorentz, γ_i is usually taken to be $\frac{1}{3}$. The static dielectric constant K, and the polarization P, are defined in terms of the electric field E, and the electric displacement D, as follows:

$$D = K\epsilon_0 E = \epsilon_0 E + P. \tag{11-2}$$

The symbols N, V, n_i, F_i, P_i, and α_i are defined as follows. N = the number of unit cells per cubic meter, $V = 1/N$ = the volume of unit cell in m^3, n_i = the number of ions of type i per unit cell, F_i = the local field at ions of type i, P_i = the contribution of ions of type i to the total polarization, and α_i = the polarizability of ions of type i, and is defined by the following equation:

$$P_i = (Nn_i)\alpha_i(\epsilon_0 F_i) \tag{11-3}$$

$$n_i\alpha_i = VP_i/\epsilon_0 F_i. \tag{11-4}$$

The success of the Clausius-Mosotti relation

$$\alpha = \sum n_i\alpha_i \tag{11-5}$$

$$= 3V(K-1)/(K+2) \tag{11-6}$$

is usually taken as evidence for the validity of the Lorentz equation. To the extent that the assumptions used in deriving these results are justified, it may be shown that the polarization P in crystals having "diagonal cubic" symmetry may be expressed in terms of the sum of the polarizabilities; thus

$$P = \sum P_i = \epsilon_0 \sum F_i\alpha_i n_i/V. \tag{11-7}$$

Assuming the same F for all ions, then

$$P = (\epsilon_0 F_i/V)\sum n_i\alpha_i = (\epsilon_0 F_i\alpha/V). \tag{11-8}$$

Making use of the additivity of α implied in Eq. (11-8) Roberts[120] has used the experimental values of α of a number of ionic crystals to prepare a table of the polarizabilities of their constituent ions. The polarizability of oxygen was arbitrarily taken to be 30 A^3, so that the resulting polarizabilities of the halide ions would be nearly proportional to their volumes.

No attempt was made to separate the total polarizabilities into their electronic and ionic components. Nevertheless, it is possible to predict within a few percent the polarizabilities of a large number of ionic cubic crystals using Robert's values of α_i.

(*a*) *Temperature dependence.*—Differentiation of Eq. (11-6) with respect to temperature leads to

$$(1/\alpha)\cdot(d\alpha/dT) = 3\cdot(1/3V)dV/dT + (3K/(K+2)(K-1))\cdot(1/K)dK/dT. \tag{11-9}$$

Thus the temperature coefficient of polarizability is the sum of the temperature coefficient of volume expansion and a term proportional to the temperature coefficient of the dielectric constant. Roberts[120] quotes the values $(1/K)dK/dT = -70\times10^{-5}$, $(1/3V)dV/dT = 0.91\times10^{-5}$ and $K = 114$ at 300°K for rutile ceramic. Substitution of these values in Eq. (11-9) yields the calculated value of $(1/\alpha)d\alpha/dT = 0.90\times10^{-5}$. This result is smaller by a factor of about 30 than the corresponding value for the alkali halides. To the extent that the Clausius-Mosotti equation can be said to apply to rutile, the large negative temperature coefficient of the dielectric constant results from the thermal expansion of rutile and the small temperature coefficient of polarizability.

(*b*) *Defect structure.*—The frequency dependence of the dielectric constant and loss angle is used to investigate the defect structure of dielectric materials. Thus Srivastava[121] has studied the defect structure in slightly impure rutile crystals. The defect structure was enhanced or modified by quenching of the crystals in liquid nitrogen after heating at 820°C for three hours in dry oxygen. The resulting absorption centers were quite anisotropic, and apparently could be observed only with the electric field in the c direction.

Below 10 kc/sec, both the real part of the dielectric constant, K', and the tangent of the loss angle, $\tan\delta$, appeared to be increasing indefinitely with decreasing

[116] W. Schmidt, Ann. Phys. **9**, 919 (1902).
[117] W. Schmidt, Ann. Phys. **11**, 114 (1903).
[118] T. Liebisch and H. Rubens, Preuss. Akad. Wiss. Ber. **8**, 211 (1921).
[119] Bunting, Shelton, and Creamer, J. Research Natl. Bur. Standards **38**, 337 (1947).
[120] Shepard Roberts, Phys. Rev. **76**, 1215 (1949).
[121] K. G. Srivastava, Progr. Rept. No. XXI (June,1957), and Progr. Rept. No. XXII (December, 1957), Laboratory for Insulation Research, Massachusetts Institute of Technology.

frequency, and exceeded the values $K'=700$ and $\tan\delta=0.7$ at 100 cy/sec. Above about 1 mc/sec, K' appeared to be asymptotic to the value for the defect-free material, and $\tan\delta$ fell off to low values.

Relaxation effects occurred in the frequency range 10 kc/sec to several megacycles a second. The frequency f_{max} at which $\tan\delta$ reached a maximum value (of approximately 0.75) increased from about 8000 cy/sec at 27°C, to about 800 kcps at 278°C. These effects could be annealed out by heating in atmospheric air at moderate temperatures (about 150°C). Measurements made below about 40°C indicated that f_{max} was an exponential function of reciprocal temperature, and the data were used to yield an estimated value of 0.18 ev for the activation energy involved.

These effects were associated with the presence of traces of silver and copper (about 0.01%), and were absent in crystals free from these impurities.

Similar phenomena have been observed by Freymann,[122] who ascribed the effect to "reorientation of positive and negative lattice defects."

(*c*) *Effect of other impurities.*—Skanavi[123,124] has found that small additions of Group II oxides to rutile cause a large increase in the dielectric constant, of the order of 3×10^4. Zerfoss and co-workers[125] believed that this might be due to the formation of an "irregular sandwich of a conducting surface region and a dielectric interior with indefinite boundaries," which would produce a large space charge polarization.

The phenomenon may be explained by the overlapping of wave functions of the more closely spaced of the impurity sites. Regions of closer than average impurity separation, would be expected to occur at random. In these regions there would be produced chains of atoms which would produce high conductivity paths of limited length. Such a mechanism would constitute a slight extension of the hypothesis of Zerfoss.

Nicolini[126] has prepared a form of ceramic "rutile" with unusual dielectric properties. The material was prepared by heating "pure' titanium dioxide to 1400°C. The dielectric constant, which has a value exceeding 10 000 at 10 cy/sec, drops to its normal value of about 100 at approximately 10^5 cy/sec. $\tan\delta$ has a maximum value of 3.2 at 20 000 cy/sec.

11.3. Optical Absorption

At 4°K, "pure" rutile is transparent in the visible region at wavelengths longer than the sharp absorption edge at 4100 A. (See Figs. 10 and 11.) This edge becomes less sharp at higher temperatures, and extends to slightly longer wavelengths. The absorption coefficient rises rapidly at wavelengths longer than 5 μ.[127,128]

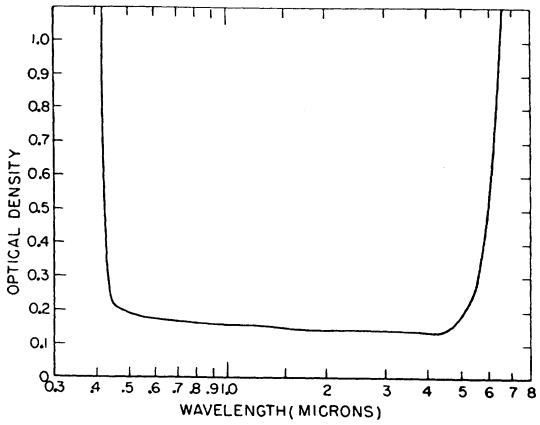

FIG. 10. Optical density of clear rutile (after Breckenridge and Hosler[128]).

After heating in hydrogen for 2.5 min at 600°C there is an increase in optical density, with a very broad maximum centered at 1.2 μ.[128]

In the far infrared, Parodi[129] found transmission lines at 30.5, 41, and 50 μ.

Breckenridge and Hosler[128] attempt to interpret the 4100-A optical edge (3.02 ev) in terms of the transition of an electron from a helium-like, neutral oxygen vacancy $(O_v\cdot 2Ti^{+3})^0$ or from a $(O_v\cdot Ti^{+3})^+$ center to the Ti^{+4} conduction band. Their assignment of the energy levels is based on evidence obtained from thermodynamics and other grounds. At higher temperatures some of these vacancies and their associated electrons are in excited states. As a result, the activation energy is supposed to be reduced and rendered less sharp.

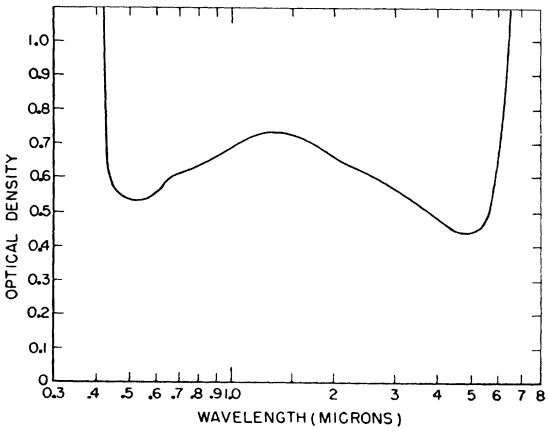

FIG. 11. Optical density of slightly reduced rutile (after Breckenridge and Hosler[128]).

[122] M. Freymann and R. Freymann, Compt. rend. **235**, 1125 (1952).
[123] G. I. Skanavi, J. Exptl. Theoret. Phys. U.S.S.R. **17**, 399 (1947).
[124] G. I. Skanavi, Doklady Akad. Nauk, S.S.S.R. **59**, 231 (1948).
[125] Zerfoss, Stokes, and Moore, J. Chem. Phys. **16**, 1166 (1948).
[126] L. Nicolini, Nature **170**, 938 (1952).
[127] D. C. Cronemeyer, Phys. Rev. **87**, 876 (1952).
[128] R. G. Breckenridge and W. R. Hosler, Phys. Rev. **91**, 793 (1953).
[129] M. Parodi, Compt. rend. **205**, 906 (1937).

Following Mott and Gurney[130] the difference between the optical and thermal activation energies (3.02 and 0.62 ev, respectively) was explained on the basis of the difference between the statical and optical dielectric constants.

Breckenridge and Hosler associate the absorption band at 1.2 μ in reduced rutile (about 1 ev with the value of 0.2 ev for the ionization potential (thermal) of the postulated donor sites $(O_v \cdot Ti^{+3})^+$. Thus the optical ionization potential of the singly ionized donor sites was believed to be five times the thermal value, consistent with the corresponding values assigned to the ionization potentials of the neutral donor (previous paragraph).

Support is claimed for this assignment of energy levels by experiments on the bleaching of colored rutile on cooling to liquid air temperatures mentioned briefly in the same paper.

11.4 Color

Weyl and Forland[131] have discussed (i) the color changes introduced by traces of ions such as Nb^{+5}, Ta^{+5}, Sb^{+5}, W^{+6}, which are usually considered colorless, and by very small traces of Fe^{+3} in rutile; (ii) the phototropy of rutile (reversible darkening when exposed to light) which may be obtained by incorporating certain impurities into rutile, as for example, a combination of the oxides of iron and niobium; and (iii) the oxidizing effect which titanium dioxide may exert on other materials when it is irradiated by ultraviolet light.

The presence of the Fe^{+3} ion introduces a rose color, that of the Nb^{+5} ion a blue-gray color into rutile. The blue-gray color is also present in reduced rutile, but unlike the effect of the Nb^{+5}, the discoloration of reduced rutile may be bleached by reoxidation.

Sandler's experiments on the rate of *ortho-para* conversion of hydrogen on the surface of rutile indicate that there is a connection between the surface paramagnetism and the blue color of lattice defects in rutile.[132] The blue color may be due entirely to a stoichiometric deficiency of oxygen in the rutile. However, Sandler points out certain inconsistencies which may indicate that the blue color is associated also with the the presence of impurities.

According to Gebhardt and Herrington,[133] the discoloration of slightly reduced rutile is due to organic contamination from stopcock grease, etc. Degassing of a "clean" sample in a "clean" vacuum system produced no discoloration. However, if either the vacuum system or the specimen were contaminated, a discoloration resulted. At temperatures of 300 to 550°C the loss of oxygen was estimated to be about 10^{-8} mole/g of TiO_2.

When heated in air to high temperatures, powdered rutile becomes lemon-yellow but returns to its original whiteness on cooling again to room temperature.[134] At 900°C there is a maximum in the emission spectrum at about 4700 A.

11.5 Refractive Indices

Measurements of the index of refraction (normal ray) in the visible region, were made by Bärwald[135] and Schroeder.[136] Cronemeyer[127] has obtained good agreement with the earlier work, and has given the result of his measurements together with values calculated from reflection measurements (Liebisch and Rubens[118]) and from transmission measurements.

Using prisms cut from single crystals, DeVore[137] has measured the refractive indices of rutile in the wavelength range 4250 to 15 000 A. DeVore has expressed his results by means of the formulas

$$n^2 = 7.197 + 3.322 \times 10^7/(\lambda^2 - 0.843 \times 10^7)$$

for the extraordinary ray and

$$n^2 = 5.913 + 2.441 \times 10^7/(\lambda^2 - 0.803 \times 10^7)$$

for the ordinary ray. The results are said to be in good agreement with those of Bärwald.[135]

Radhakrishnan[138] has used the method of Bragg to calculate the refractive indices of rutile. This worker has also used the measurements of Schroeder[136] to derive the values of the constants a, b, c, and λ_0 in the dispersion formula for rutile

$$n^2 - 1 = a - c\lambda_0^2 - b\lambda^2/(\lambda^2 - \lambda_0^2)$$

in which n is the index of refraction at wavelength λ. Values calculated using this relation agreed with observation within the experimental error.

11.6 Reflection Coefficient

The reflection coefficient of natural rutile crystals has been measured by Liebisch and Rubens[118] in the range 1.4 to 300 μ. Their results appear in Fig. 12.

12. ADSORPTION AND SURFACE LAYERS

In this section no reference is made to the extensive literature concerning adsorption of various gases and vapors on rutile powder, with the exception of certain experiments which yield direct information concerning the defect structure of the surface of rutile.

From the measured rate of *ortho-para* conversion of hydrogen at the surface of rutile (discussed also in

[130] N. F. Mott and R. W. Gurney, *Electronic Processes in Ionic Crystals* (Oxford University Press, New York, 1948).
[131] W. A. Weyl and Tormod Forland, Ind. Chem. **42**, 257 (1950).
[132] Y. L. Sandler, J. Phys. Chem. **58**, 54 (1954).
[133] J. Gebhardt and K. Herrington, J. Phys. Chem. **62**, 120 (1958).
[134] G. I. Sinyapkina, Zhur. Eksptl. i Teoret. Fiz. **19**, 581 (1949).
[135] W. Bärwald, Z. Krist. **7**, 168 (1883).
[136] A. Schroeder, Z. Krist. **67**, 485 (1928).
[137] J. R. DeVore, J. Opt. Soc. Am. **41**, 416 (1951).
[138] T. Radhakrishnan, Proc. Indian Acad. Sci. **A35**, 117 (1952).

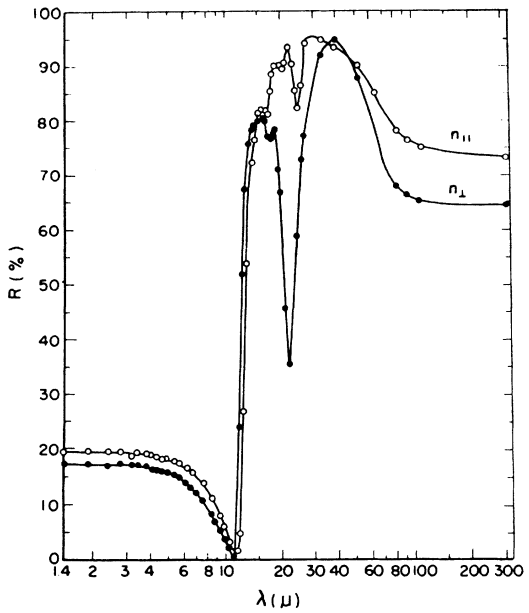

FIG. 12. Reflection coefficient in percent for natural single crystals of rutile (after Liebisch and Rubens[118]).

Sec. 11.4), Sandler[139] has obtained information concerning the state of adsorbed oxygen. The oxygen adsorbed on rutile at 90°K is apparently in molecular form, and the correspondingly high conversion rate is ascribed to the paramagnetism of this form of oxygen. On heating the specimen to room temperature, dissociation of some of the oxygen evidently occurred, leading to re-oxidation of the surface and a disappearance of the blue color. Reyerson and Honig[140] have investigated the diamagnetic susceptibility of NO_2-N_2O_4 adsorbed on rutile. To obtain a constant value for the gram susceptibility of the absorbate these workers found it necessary to assume that the (positive) susceptibility of the rutile decreased during adsorption. Thus it seemed reasonable to suppose that the rutile was initially partially reduced, but became re-oxidized by the NO_2-N_2O_4. The true value (after re-oxidation) of the susceptibility of rutile estimated in this way was 0.061×10^{-6} cgs units per gram. This interpretation is strengthened by the observed permanent increase in weight of the specimen, and by spectroscopic analysis of the equilibrium gases.

12.1. Photoconductivity in Surface Layers

The curves of spectral distribution of photoconductivity of most semiconductors exhibit a sharp rise in the vicinity of the absorption edge. As the wavelength of the incident light decreases, the response reaches a maximum value, and begins to decrease while the absorption coefficient is still rising. At small intensities the photocurrent is usually proportional to the light intensity at all wavelengths.

On the long wavelength side of the response maximum, the absorption coefficient is small, and much of the incident radiation traverses the crystal without being absorbed. On the short wavelength side, the penetration depth is small, and most of the absorption takes place in the surface region, where the electron recombination velocity†† is high. The wavelength of maximum response is determined by the relative importance of these mechanisms. Thus the response maximum will depend on the thickness of the crystal, and on the temperature, if the absorption coefficient is temperature-dependent.

Cronemeyer[127] has measured the photocurrent of thin crystals of rutile as a function of the wavelength of the incident radiation. The response increased rapidly with the energy of the incident photons in the region of 2.9 ev (4300 A). The edge of the photoconductivity curve is shifted to slightly lower energies as the temperature is increased from 103 to 295°K. Because of the high absorption coefficient above 3 ev (4100 A), and because of the important role of surface effect in this region, the interpretation of the results is difficult for higher photon energies.

At 1.2 μ, the response is smaller than the maximum response by a factor of 10^6.

13. BAND STRUCTURE OF RUTILE—CONCLUSIONS

Estimates of the width of the energy gap from measurements of electrical conductivity in the intrinsic range involve an assumption that the density-of-states effective masses of the valence and conduction bands are identical.

The measurements of electrical conductivity made in the high temperature range (700 to 1100°C) where presumably the intrinsic conductivity is measured, indicate that the forbidden energy gap of rutile is between 3 and 4 ev. The experimental value obtained by Earle (3.4 ev), Hauffe (3.9 ev), and Cronemeyer (3.06 ev) are discussed in another section. Cronemeyer's investigation of optical absorption and photoconductivity yield a value of about 2.8 to 3.1 ev.

The sign of the charge carriers in semiconductors is usually obtained from Hall or thermopower measurements. Because of the difficulty of measuring the potential at a point on the surface of a high resistance specimen, Hall measurements have not been made on specimens of rutile in the intrinsic range. Measurements of thermopower on rutile specimens of high purity indicate that the charge carriers are probably electrons.

The measurements of Breckenridge and Hosler

[139] Y. L. Sandler, J. Phys. Chem. **58**, 54 (1954).
[140] L. H. Reyerson and J. M. Honig, J. Am. Chem. Soc. **75**, 3920 (1953).

†† The surface recombination velocity is defined as "the rate at which electrons disappear from the interior across the surface, divided by the density of electrons in excess of equilibrium in the interior."

indicate that the mobility of reduced specimens is about 0.1 cm^2 $volt^{-1}$ sec^{-1} at 500°K. The value for intrinsic rutile may be approximately the same. By combining this value of mobility with the electrical conductivity measurements of Cronemeyer, one obtains an effective electron mass ratio of the order of 1000. However, values of the electron concentration evaluated from the combined Hall and conductivity data of Breckenridge and Hosler (see Sec. 8) yield effective mass ratios of the order of unity.

An attempt has also been made to discuss the band structure of reduced rutile with the inclusion of a donor band. The measurements of the magnetic susceptibility of rutile containing a stoichiometric deficiency of oxygen made by Ehrlich could be explained by the presence of such a donor band approximately 0.04 ev in width. Assuming the existence of this band (in which the mobility is expected to be low, and the effective electron mass high), then the donor band is probably 0.05 to 0.20 ev below a "conduction band" (in which the effective mass is considerably lower). The values of the energy separation of these bands calculated from the conductivity, Hall effect, and thermopower measurements discussed in earlier sections are given after the author's names. Electrical conductivity of reduced rutile: Kataoka and Suzuki (0.12 to 0.15 ev). Thermopower: Kataoka and Suzuki (0 to 0.13 ev). Hall data: Breckenridge and Hosler (0.025 to 0.05 ev). Optical absorption: An absorption band characteristic of reduced rutile was observed by Cronemeyer in the range 1 to 3 μ (0.4 to 1.2 ev). In order to compare these energies with the other data, they may have to be reduced by a factor of about 5.1 to allow for the difference between the optical and statical dielectric constants, as discussed in Sec. 11.3. This correction would place the donor band about 0.08 to 0.24 ev below the conduction band.

The evidence for the presence of a donor band is not conclusive. Consequently, the data have also been discussed below in terms of noninteracting sites. On the basis of the simple model and the assumption of noninteracting donor sites, the electrical conductivity measurements lead to the values of donor ionization potentials: Kataoka and Suzuki (0.29 to 0.35 ev), Boltaks (less than 0.2 ev). Thermopower: Kataoka and Suzuki (0.02 to 0.13 ev); Henisch (0.09 ev). Hall measurements: Breckenridge and Hosler (0.10 to 0.15 ev).

14. THERMODYNAMIC PROPERTIES AND REDUCTION

14.1. Thermodynamic Properties

The thermodynamic properties, free energy of formation, etc., of the various oxides (and many other compounds of titanium) are fully listed in the publication: The Properties of Titanium Compounds and Related Substances, ONR Report ACR-17 (October, 1956). These tables were prepared from the results of Humphrey,[141] Mixter,[142] Sieverts and Gotta,[143] Roth and Becker,[144] Neumann *et al.*,[145] Roth and Wolf,[146] Foëx,[147] Kelley,[148] Shomate,[149] Naylor,[150] and others. Brewer[151] has prepared a review of the thermodynamic properties of metallic oxides, including the various oxides of titanium. These properties enable one to estimate an upper limit for the free energy of formation of an oxygen vacancy in rutile. We are chiefly interested in departures from stoichiometry so small that the rutile structure is maintained and lower oxides such as Ti_3O_5 are not present as separate phases.

14.2. The Reduction of Rutile

X-ray studies[80,152] show that the rutile structure is maintained even for a weight loss as great as two percent (composition $TiO_{1.90}$). When the weight loss is somewhat greater than this value, the lower oxide Ti_3O_5 (or Ti_2O_3) forms as a separate phase, depending on the temperature.

The pressure of oxygen in equilibrium with titanium oxide decreases with the degree of reduction, the decrease being most rapid when the composition is close to the relative oxygen content represented by the formulas Ti_2O_3, Ti_3O_5, and TiO_2. For values of weight loss up to two percent, the degree of reduction may apparently be controlled[163] by heating the specimen of rutile in oxygen at reduced pressure, in a vacuum system free from contamination by stopcock grease. For high degrees of reduction, the equilibrium oxygen pressure is inconveniently low for the use of this simple method, and it becomes necessary to reduce the specimen by chemical means.

The oxygen pressure may be established at the desired low value by heating the specimen in a mixture of hydrogen and water vapor of known composition. The equilibrium constant of this reaction is known with accuracy,[153] and the equilibrium oxygen pressure may be calculated from the following equation:

$$\log K_p = \log p_{O_2} (p_{H_2}/p_{H_2O})^2 = 5.9 - 25\,900/T.$$

Alternatively, the CO-CO_2 reaction may be used to establish the desired oxygen pressure around the specimen.[152] A third method involves the heating of the titanium oxide in a sealed container with some

[141] G. L. Humphrey, J. Am. Chem. Soc. **73**, 1587 (1951).
[142] W. G. Mixter, Am. J. Sci. **27**, 393 (1909).
[143] A. Sieverts and A. Gotta, Z. anorg. u. allgem. Chem. **199**, 384 (1931).
[144] W. A. Roth and G. Becker, Z. physik. Chem. **A159**, 1 (1932).
[145] Neumann, Kröger, and Kunz, Z. anorg. u. allgem. Chem. **218**, 379 (1934).
[146] W. A. Roth and U. Wolf, Rec. trav. chim. **59**, 511 (1940).
[147] M. Foëx, Bull. soc. chim. **11**, 6 (1944).
[148] K. K. Kelley, U. S. Bur. Mines Bull. 383 (1935).
[149] C. H. Shomate, J. Am. Chem. Soc. **69**, 218 (1947).
[150] B. F. Naylor, J. Am. Chem. Soc. **68**, 1077 (1946).
[151] L. Brewer, Chem. Revs. **52**, 1 (1953).
[152] Assayag, Dode, and Faivre, Compt. rend. **240**, 1212 (1955).
[153] F. D. Richardson and J. H. E. Jeffes, J. Iron Steel Inst. (London) **160**, 261 (1948).

pieces of a metal which forms a very stable oxide. Experiments in which these methods have been used are discussed in the following.

14.2.1. Heating in Oxygen at Reduced Pressure

Assayag *et al.*[152] have measured the equilibrium oxygen pressure and the corresponding weight loss when rutile is heated in oxygen to temperatures above 1000°C.‡‡ Little information was given concerning the vacuum system used. Because of the possibility of contamination by stopcock grease, and the presence of CO in the vacuum system, the results should be accepted with caution.

Gebhardt and Herrington[154] obtained the usual discoloration when rutile was degassed for sixteen hours at 400 to 600°C in a conventional vacuum system, using greased stopcocks. However, when a sample was cleaned by heating in oxygen before degassing in a clean system, this discoloration was not obtained. These workers believe that the discoloration results from contamination of the rutile by organic impurities originating in the stopcock grease. The "clean" vacuum system made use of a mercury diffusion pump and mercury cutoffs instead of stopcocks. The conclusions were substantiated by mass spectrometric analysis and the detection of CO and CO_2 in the vacuum system.

14.2.2. Use of the CO-CO_2 *Equilibrium*

Assayag *et al.*[152] have used the equilibrium between CO and CO_2 to control the degree of reduction of rutile corresponding to compositions in the range $TiO_{1.908}$ to $TiO_{1.977}$ (i.e., 0.4% to 2% loss in weight). They have also shown by x-ray methods that this material retained the rutile structure.

14.2.3. Use of the Hydrogen-Water Vapor Equilibrium

Nasu[155–157] has used the hydrogen-water vapor equilibrium in the reduction of rutile in the temperature range 1022 to 1282°K. A specimen of powdered rutile was placed in a platinum crucible and suspended in an iron reaction chamber at the end of a quartz spring. The approach to equilibrium could be determined by the change in weight. A mixture of hydrogen and water vapor of unstated composition was introduced to the specimen. Later the composition of a sample of the equilibrium mixture was determined by measuring its pressure with a McLeod gauge both before and after the removal of the water vapor by condensation with liquid nitrogen, and the ratio of the partial pressures in the equilibrium mixture was then calculated.

Nasu[155–157] found that the equilibrium oxygen pressure remained constant from one percent to about 9.7% reduction, at which point its value fell abruptly. The absence of variation in the equilibrium constant in this range of reduction seems to indicate that the lower oxide existed as a separate phase, and the value of 9.7% corresponds closely to the loss in weight corresponding to the formation of Ti_2O_3. These results seem to set an upper limit of one percent to the weight loss which rutile can sustain at these temperatures without leading to the presence of aggregates of a different phase, i.e., when speaking of slightly reduced rutile, a weight loss of less than one percent is implied.

Unfortunately, the equilibrium ratios calculated from more recent calorimetric and free energy data are considerably higher than Nasu's values. Moreover, as Kelley has pointed out, Nasu's high-temperature data correspond exactly to the p_{H_2O}/P_{H_2} ratio for the FeO-Fe system, which fact may be related to Nasu's use of an iron reaction chamber.

14.2.4. Use of the Alkaline Earth Metals

Kubaschewski and Dench[158] have investigated the partial free energy of the titanium-oxygen system at 1000 and 1200°C between the limits of zero and 38% oxygen by weight. A quantity of barium, calcium, or magnesium was mixed with a quantity of one or other of the oxides of titanium. The mixture was sealed in a steel container and fired at the desired temperature. After cooling, the alkaline earth oxide was dissolved with hydrochloric acid and the remaining powder was analyzed for O; N, H, Fe, Ba, Ca, or Mg, and Ti. The equilibrium oxygen pressure was assumed to be that of the alkaline earth oxide at the temperature of the reaction. From these data a plot was made of partial free energy against composition of the oxide. In this paper, the effect of the formation of alkaline earth titanate was not discussed. The pressure of oxygen in equilibrium with a quantity of alkaline earth titanate is probably lower than that in equilibrium with the alkaline earth oxide.

14.2.5. Other Methods

Ehrlich[80] prepared specimens of TiO_x with x greater than 1.97 by heating appropriate mixtures of rutile and titanium metal or TiO to 1500–1600°C. Wyss[159] investigated the reduction of rutile by hydrogen and reported that at 1575°K, Ti_3O_5 is formed. The absence of further reduction under these conditions seems to indicate, as pointed out by Brewer,[151] that Ti_2O_3 is

‡‡ In the temperature range $T=1318$ to 1531°K, and $p=10^{-2}$ to 10^{-4} atmos, the results of these workers may be expressed very roughly by the following expression for the fractional weight loss f.

$$\log f = -\tfrac{1}{5}\log p_{O_2} - 5000/T - 0.10.$$

[154] J. Gebhardt and K. Herrington, J. Phys. Chem. **62**, 120 (1958).
[155] Nobuyuki Nasu, Sci. Repts. Tôhoku Univ. **12**, 371 (1935).
[156] Nobuyuki Nasu, J. Chem. Soc. (Japan) **56**, 659 (1935).
[157] Nobuyuki Nasu, Sci. Repts. Tôhoku Univ. **XXV**, 510 (1936).
[158] Kubaschewski and Dench, J. Inst. Metals **82**, 87 (1953).
[159] R. Wyss, Ann. chim. **3**, 215 (1948).

more stable relative to Ti_3O_5 than Humphrey's data appear to indicate.[141]

Kelley has investigated the reduction of rutile in an atmosphere of hydrogen-water vapor, but his results have not been published. As reported by Brewer,[151] the equilibrium pressure ratio p_{H_2O}/p_{H_2} changes abruptly at the composition Ti_3O_5. On the other hand, Welch[160] found no evidence for Ti_3O_5 when rutile is reduced by hydrogen at 1400°K. At 1700°K, Ti_3O_5 can be formed, in confirmation of Humphrey's conclusion that Ti_3O_5 is stable only at high temperatures.

Russian workers have investigated the reduction of metal oxides by hydrogen, and by alcohols.[161] Freundlich and Bichara[162] have used CaH_2 to reduce rutile. In his paper "Reduction of metallic oxides by carbon in boric oxide and borax melts," Khundkar[163] reports that rutile is not reduced by active carbon at 1000°C.

[160] A. J. E. Welch, 120th Meeting of the American Chemical Society, New York (September, 1951).

[161] V. A. Komarov, Uchenye Zapiski Leningrad Univ. No. 169, Ser. Khim. Nauk No. **13**, 29–35 (1953).

[162] W. Freundlich and M. Bichara, Compt. rend. **238**, 1324 (1954).

ACKNOWLEDGMENTS

The writer is grateful to A. D. Franklin, H. P. R. Frederikse, H. S. Peiser, and J. B. Wachtman, Jr., of the National Bureau of Standards, who have read the manuscript, and have made numerous valuable suggestions.

Acknowledgment, with thanks, is extended to the following authors and journals for permission to use their diagrams: L. Pauling and the Cornell University Press for Fig. 2. W. H. Baur and Acta Crystallographic for Fig. 3. H. P. Hanson, J. R. Knight, and the Physical Review, for Fig. 4. R. G. Breckenridge, W. R. Hosler, and the Physical Review, for Figs. 1, 8, 9, 10, and 11. T. Liebisch, H. Rubens, and die Deutsche Akademie der Wissenschaften for Fig. 12.

[163] M. H. Khundkar, J. Indian Chem. Soc. **29**, 467 (1952).